

國立交通大學

光電工程研究所

碩士論文

介電層氫氧基對五苯環有機薄膜電晶體
的影響



**Dielectric Hydroxyl Groups Effects in
Pentacene-based OTFTs**

研究生：孟繁琦

指導教授：冉曉雯 博士

中華民國九十八年七月

Chinese Abstract

介電層氫氧基對五苯環有機薄膜電晶體的影響

研究生：孟繁琦

指導教授：冉曉雯

國立交通大學

光電工程研究所碩士班

摘要

有機薄膜電晶體相對於傳統的非晶矽薄膜電晶體有許多優點，如：低溫製程、低成本、可撓性…等，但於此同時，元件可靠度低和壽命短則是其應用上最大的弱點。缺陷捕捉載子是目前公認造成有機薄膜電晶體臨界電壓飄移和遷移率裂化的最主要原因。

此論文主要研究有機薄膜電晶體中氫氧基受環境影響而產生缺陷的機制。我們使用聚甲基丙烯酸甲酯(PMMA)和聚乙炔酚(PVP)做為介電層表面處理材料，做出二種不同的有機薄膜電晶體，其中 PVP 處理的表面存在有氫氧基。

首先由光環境和暗環境中量測二種元件的遲滯效應，推論氫氧基應該可以形成捕捉電子的缺陷，而照光則會在有機半導體中產生電子電洞對，提供被捕捉電子的來源。接著比較二種元件在光環境和暗環境中做閘極正偏壓實驗，推論閘極正偏壓會導致有機半導體能帶彎曲，使原來不被填滿的缺陷態傾向被光產生的電子填滿，造成臨界電壓飄移。真空環境中閘極正偏壓的量測進一步說明，氫氧基要形成電子缺陷，應該是需要與大氣中的水氣和氧氣結合才行，此種缺陷不論是在光環境或是暗環境下，都會造成臨界電壓飄移。

針對以上缺陷產生的機制，設計適當保護層可以使有機薄膜電晶體更進一步朝向實用化。相反的，氫氧基使元件特性對水氧有明顯的變化，說明了有機元件

在水氣和光偵測器上應用的可能性。



English Abstract

Dielectric Hydroxyl Groups Effects in Pentacene-based OTFTs

Student : Fan-Chi Mong

Advisor : Hsiao-Wen Zan

Institute of Electro-Optical Engineering National Chiao Tung

University

Abstract

Organic thin film transistors compared with the conventional amorphous silicon thin film transistors have many advantages, such as: low-temperature process, low cost, flexible ... and so on. However, poor reliability and short life time is its application greatest weaknesses. So far, carrier capture defects are recognized as the main reason that causes threshold voltage shift and mobility degradation.

In this thesis, dielectric hydroxyl groups (OH groups) defects forming mechanism influenced by the environment is studied. We use methyl methacrylate (PMMA) and poly-4-vinyl phenol (PVP) as the dielectric surface treatment material and make two kinds of OTFTs. PVP-OTFTs have OH groups on its interface while PMMA-OTFTs do not.

By comparing PMMA and PVP devices' hysteresis in dark and under light, we find OH groups can form defects and trap electrons. Illumination will photogenerate electron-hole pair in the organic semiconductor and provides the source of trapped electrons. Then, PMMA and PVP devices positive gate bias stress experiment in dark/light environment indicated that positive gate bias stress can make semiconductor's energy band bending, some originally do not filled defect states will tend to trap photogenerated electrons and thus cause threshold voltage shift.

In addition, positive gate bias stress experiment taken in vacuum environment

further proved OH group should react with H₂O and O₂ in the air then electron defects could be formed. OH groups defects can cause threshold voltage shift on matter it was in dark or light environment.

In order to realize OTFTs' application, passivation layer that could protect organic semiconductor from environment effect is needed. On the other hand, significant threshold voltage shift caused by OH groups implicate OTFTs application on moisture/light sensor.



Acknowledgement

碩士二年很快的過去，實驗可以順利完成並寫出論文，首先要感謝指導教授冉曉雯老師還有帶我的博班學長高士欽，實驗方向和實驗方法因為有他們的指引，才能有更嚴謹的邏輯和架構，而論文的文法也才能更為通順。

另外要感謝二年來一起實驗的同伴，讓我在奈米中心無塵室製作元件、4156量測電性、材料分析的時光不孤單無聊。碩一時有方哥不知道在兇什麼但是很搞笑的實驗指導，讓我雖然做元件失敗但覺得人生還是充滿希望，另外顏哥志宇不務正業的課外休閒，也讓我在緊湊的實驗中看到不同專業領域的世界。使用 4156 時，和進進出出戴老師、劉老師的同學們討論交映樓的八掛，是深夜裡量測歡笑的來源。很會搞笑的小寶，樂觀的淑玲，冷靜的歐陽，自強不息的自強，古錐的玉玫，憨厚的達欣，討人厭的王建敏，有擔當的小哈，社交真的極其廣泛到讓我不知該如何表達對其景仰的威豪，帥氣的賣摳，零食很多愛幫助人的慶能，是這二年研究路上不能沒有的，酒肉上和精神層次上好夥伴。

竟然貼心送我們畢業卡片的學弟妹們：研究生涯就和他做的元件一樣會一直飄移的許五百，辛勤認命的明哲，好像很胡塗的羅世益，有很多飲料可以喝的琇文，老成的唯碩，像優雅公子的建亞，會照相又懂音樂的翼鵬，熱心溫順的宏榮，認真的柏翔。謝謝你們處理了不少雜事，讓我們能無後顧之憂的做研究，希望你們明年也可遇到一樣好的學弟妹幫忙順利畢業。

另外，清大材料的同學，羅浮的夥伴，也都提供我許多實質上和心靈上的幫助，套句紅茶的話”能有辛畢業，都是大家的功勞”。

最後，謹以此文獻給我摯愛的雙親。

Contents

| | |
|---|-----|
| Chinese Abstract | I |
| English Abstract | IV |
| Acknowledgement | VI |
| Contents | VII |
| Table Captions | IX |
| Figure Captions | X |
| Chapter 1 | 1 |
| 1.1 An Overview of Pentacene-Based Thin-Film Transistor | 1 |
| 1.2 Operation of OTFTs | 2 |
| 1.3 Defect Generation Mechanism | 3 |
| 1.3.1 Threshold Voltage Shift Mechanism | 4 |
| 1.3.2 Resources of trapped carrier | 5 |
| 1.3.3 Field-Effect Mobility Degradation | 6 |
| 1.4 Surface Treatment | 6 |
| 1.5 Motivation | 7 |
| Figure of Chapter 1 | 8 |
| Chapter 2 | 9 |
| 2.1 Device Fabrication | 9 |
| 2.2 Material Analysis Instrument | 11 |
| 2.2.1 Contact angle system | 11 |
| 2.2.2 Fourier Transform Infrared Spectroscopy (FTIR) | 11 |
| 2.2.3 X-Ray Diffraction (XRD) | 12 |
| 2.2.4 Atomic force microscope (AFM) | 12 |
| 2.3 Device Electrical Characteristic Measurement | 13 |
| 2.4 Illumination Setup | 13 |

| | |
|---|-----------|
| 2.5 Device Electrical Parameters Extraction | 14 |
| 2.5.1 Field Effect Mobility | 14 |
| 2.5.2 Threshold voltage | 15 |
| Figure of Chapter 2..... | 16 |
| Table of Chapter 2 | 22 |
| Chapter 3 | 23 |
| 3.1 Material Analysis of PVP and PMMA | 23 |
| 3.1.1 Wettability of PVP and PMMA Dielectrics | 23 |
| 3.1.2 FTIR of PVP and PMMA Dielectrics..... | 23 |
| 3.2 Electric Transfer Characteristics of Devices with PVP and PMMA Dielectrics..... | 24 |
| 3.2.1 XRD Analysis of PVP and PMMA Dielectrics..... | 25 |
| 3.2.2 Morphology of PMMA, PVP and Pentacene Films | 26 |
| 3.2.3 Hysteresis | 26 |
| 3.3 Bias Stress and Hydroxyl Groups Influence on the Device Threshold Voltage..... | 27 |
| 3.3.1 Bias Stress in Dark Environment | 28 |
| 3.3.2 Bias Stress under Illumination..... | 30 |
| 3.3.3 Bias Stress in Vacuum Environment..... | 32 |
| 3.3.4 Different Light Wavelength Influence | 33 |
| Figure of Chapter 3..... | 35 |
| Chapter 4 | 47 |
| Reference | 49 |

Table Captions

TABLE 2.1 PMMA AND PVP SPIN COATING PARAMETERS22



Figure Captions

| | | |
|------------|--|----|
| FIG. 1. 1 | PENTACENE MOLECULAR STRUCTURE | 8 |
| FIG. 1. 2 | OTFT DEVICE CONFIGURATIONS. (A) CROSS SECTION VIEW OF TOP | 8 |
| FIG. 2. 1 | PMMA MOLECULAR STRUCTURE..... | 16 |
| FIG. 2. 2 | PVP MOLECULAR STRUCTURE..... | 16 |
| FIG. 2. 3 | SCHEMATIC PICTURE OF MMF CROSS-LINK WITH PVP..... | 17 |
| FIG. 2. 4 | SCHEMATIC STRUCTURE OF PVP-OTFTS AND PMMA-OTFTS..... | 17 |
| FIG. 2. 5 | IMAGE OF CONTACT ANGLE SYSTEM..... | 18 |
| FIG. 2. 6 | ABSORBANCE SPECTRUM OF DIFFERENT FUNCTION GROUPS | 18 |
| FIG. 2. 7 | PICTURE OF SHIMADZU XRD-6000 | 19 |
| FIG. 2. 8 | PICTURE OF DIGITAL INSTRUMENTS D3100..... | 19 |
| FIG. 2. 9 | PICTURE OF VACUUM CHAMBER | 20 |
| FIG. 2. 10 | INTENSITY OF LED (RED, GREEN ,BLUE AND WHITE) WAVELENGTH SPECTRUM..... | 21 |
| FIG. 3. 1 | MOISTURE CONTACT ANGLE OF PVP AND PMMA DIELECTRIC | 35 |
| FIG. 3. 2 | FTIR SPECTRA OF PVP AND PMMA FILM..... | 35 |
| FIG. 3. 3 | THE INITIAL TRANSVERSE CHARACTERISTIC OF PVP-OTFTS AND | 36 |
| FIG. 3. 4 | X-RAY DIFFRACTION (XRD) PATTERN OF PENTACENE DEPOSIT ON PVP AND..... | 36 |
| FIG. 3. 5 | ATOMIC FORCE MICROSCOPE (AFM) IMAGES OF (A)PMMA SURFACE (B) PVP SURFACE, AND IMAGES OF 25 Å PENTACENE (C) DEPOSIT ON PMMA DIELECTRIC (D) DEPOSIT ON PVP DIELECTRIC | 37 |
| FIG. 3. 6 | THE TRANSFER CHARACTERISTIC OF PVP-OTFTS SWEEP IN BOTH DIRECTIONS | 38 |
| FIG. 3. 7 | THE TRANSFER CHARACTERISTIC OF PMMA-OTFTS SWEEP IN BOTH..... | 38 |
| FIG. 3. 8 | THE LINEAR-REGION TRANSFER CHARACTERISTICS OF DEVICES BEFORE | 39 |
| FIG. 3. 9 | THRESHOLD VOLTAGE SHIFT (ΔV_{TH}) OF PMMA AND PVP DEVICES DURING | 39 |
| FIG. 3. 10 | THE FIELD-EFFECT MOBILITY PLOT AS A FUNCTION OF POSITIVE BIAS STRESS | 40 |
| FIG. 3. 11 | THE LINEAR-REGION TRANSFER CHARACTERISTICS OF DEVICES BEFORE..... | 40 |
| FIG. 3. 12 | THRESHOLD VOLTAGE SHIFT (ΔV_{TH}) OF PMMA AND PVP DEVICES DURING | 41 |
| FIG. 3. 13 | THE FIELD-EFFECT MOBILITY PLOT AS A FUNCTION OF NEGATIVE BIAS STRESS..... | 41 |
| FIG. 3. 14 | THRESHOLD VOLTAGE SHIFT (ΔV_{TH}) OF PMMA AND PVP DEVICES UNDER | 42 |
| FIG. 3. 15 | THE LINEAR-REGION TRANSFER CHARACTERISTICS OF DEVICES BEFORE AND | 42 |
| FIG. 3. 16 | THRESHOLD VOLTAGE SHIFT (ΔV_{TH}) OF PMMA AND PVP DEVICES IN..... | 43 |
| FIG. 3. 17 | MODEL OF THRESHOLD VOLTAGE SHIFT CONTROLLED BY THE CHARGE CAPTURING..... | 43 |
| FIG. 3. 18 | LONG TIME POSITIVE BIAS STRESS EXPERIMENT OF PVP-OTFTS IN DARK | 44 |

FIG. 3. 19 THRESHOLD VOLTAGE SHIFT (ΔV_{TH}) OF PMMA AND PVP DEVICES IN DARK 44
FIG. 3. 20 THRESHOLD VOLTAGE SHIFT (ΔV_{TH}) OF PMMA AND PVP DEVICES IN DARK 45
FIG. 3. 21 THRESHOLD VOLTAGE SHIFT (ΔV_{TH}) OF PMMA AND PVP DEVICES UNDER 45
FIG. 3. 22 THE ABSORPTION SPECTRUM OF PENTACENE ON PVP AND PMMA FILM 46



Chapter 1

INTRUDUCTION

1.1 An Overview of Pentacene-Based Thin-Film Transistor

Recently, organic thin-film transistors (OTFTs) have received great attention due to their low-cost and large-area array application. In numerous organic materials, pentacene is promising candidate due to its high mobility. Pentacene is made up of five benzene rings as shown in Fig. 1.1.


In previous studies, there are many superior groups to promote the electrical characteristic of pentacene-based thin-film transistors such as field-effect mobility, subthreshold slope, I_{on}/I_{off} ratio, and low operation voltage.

OTFT arrays to drive liquid crystal (LC) [1][2] or organic light emitting diode (OLED) [3] which showed full-color moving pictures had been demonstrated. In these reports, OTFTs were encapsulated by passivation layer to avoid exposing to oxygen or moisture in air, and to avoid damage from the subsequent LC or OLED process. However, even when devices are encapsulated or operated in an inert environment, OTFTs are known to suffer from bias stress effect (BSE) that causes significant threshold voltage shift.

The bias-stress effect in OTFTs had been studied by using different organic active materials or different gate insulators on different device structures [4]. It was found that, for p-type OTFTs under DC stress, positive gate bias stress caused a positively-shifted V_{th} and negative gate bias stress caused a negatively-shifted V_{th} . The BSE was reversible by removing gate bias or by applying opposite polarity gate bias. Light irradiation also enhanced the reversal process.

Charge trapping, ion migration, charged-state creation and the formation of bound hole pairs (bipolaron) are several proposed mechanisms to explain the BSE [5]. Charge trapping and ion migration were found to be dominant mechanisms in OTFTs with an organic dielectric [6]. When using thermally-grown SiO₂ as the gate dielectric to study OTFTs reliability, charged-state creation is usually believed to be responsible for ΔV_{th} . John E. Northrup and Michael L. Chabinyk used density functional calculation to simulate defect states generation in pentacene film and found that it was due to the formation of oxygen- and hydrogen-related defects such as C-H₂, O_H, and C-HOH in organic semiconductors [7]. Gu et al. also studied the response time of the defect states in pentacene. Long-lifetime deep electron traps were proposed to explain the hysteresis effect in pentacene-based OTFTs.

1.2 Operation of OTFTs



A thin film transistor is composed of three basic elements: (i) a thin semiconductor film; (ii) an insulating layer; and (iii) three electrodes (source, drain and gate). Fig.1.2 show two kinds of standard OTFT device structure Fig. 1.2(a) is the top-contact device and Fig. 1.2(b) is the bottom-contact device, respectively. The general operation concepts are originated from MOSFET theory. But there is a slight difference, traditional MOSFET are usually operated in inversion mode while the OTFTs are generally operating in accumulation mode.

Since the pentacene is a p-type semiconductor, negative bias is applied on the gate to turn on our OTFTs. The voltage-drop across dielectric causes the energy band bending in the organic semiconductor and additional positive charge carriers will accumulate at the interfaces. The dielectric serves as a capacitance and can store charges. Then we apply a drain bias to drive the accumulated charges from source to drain and from the drain current. The conduction is determined by the field effect

mobility (μ_{FE}) which represents charges' driving ability by the electrical field.

In general, we can divide the operation of OTFTs into two regions: linear region and saturation region. If we add gate bias at turn on state, beginning with small drain voltage, OTFTs are operated in linear region, as given drain become larger the drain current will gradually saturate and into saturation region.

Understand how OTFTs normally operate, parameters such as the threshold voltage, field effect mobility can be extracted according to the measured electric characteristic. In addition, how environment effect devices can also be told by analyzing abnormal changing of these parameters.

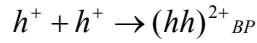
1.3 Defect Generation Mechanism

Until now, the device reliability issue has been a greatest barrier to realize the organic electronic application. Even when devices are encapsulated, the threshold voltage (V_{th}) tends to shift under continuous bias and the field effect mobility degrades after prolonged storage in normal environment. The device threshold voltage shift (ΔV_{th}) is generally attributed to hole/electron trapping in the interface between pentacene and dielectric. Although the field effect mobility degradation mechanism is not clearly understood, the permeation of H_2O and O_2 in pentacene film is the usually proposed mechanism. These two phenomena seriously strict the organic TFTs application ranges. Therefore, in following section, mechanisms caused device ΔV_{th} and field effect mobility degradation are explained in detail

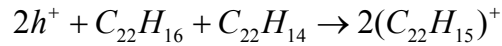
1.3.1 Threshold Voltage Shift Mechanism

The ΔV_{th} of OTFTs is believed due to the carrier trapping by the defect states. However, there are only a few explanations on the micro process of the defect creation, which can be observed in bias stress experiment. Bias stress experiment can be divided into two kinds: negative bias stress and positive bias stress.

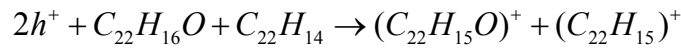
First, micro process of defect creation under negative bias stress is introduced. The formation of bipolaron proposed by R. A. Street et al. (Phys. Rev. B, vol.68, 085316, 2003) is one of the plausible mechanisms. The deep states slowly trap holes to form bipolarons. The formation of bipolarons would cause the ΔV_{th} due to the reduction of mobile holes. The reaction can be expressed as:



The other possible mechanism was proposed by John John E. Northrup et al. (Phys. Rev. B, vol.68, 041202, 2003) They studied the formation of hydrogen- and oxygen-related defects (C-H₂, O_H, and C-HOH) in pentacene film based on the density functional calculation. The defect creation reactions were given as follows:



and

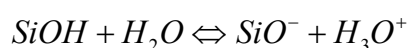


When the pentacene film is in a hole-rich environment, both these two reactions tend react to the right-hand side and produce positive-charged states that cause the ΔV_{th} . Either bipolaron formation or hydrogen-, oxygen-related defect creation, these studies need more experimental results to support their theories. Both mechanisms assume that the reaction rate is proportional to the carrier concentration.

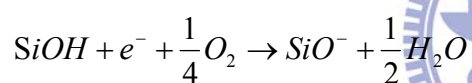
However, compare with negative bias stress effect, there are fewer studies focused on positive bias stress effect. Applying a prolonged positive bias to the device usually

causes electrons trapping in the channel and a threshold voltage shift forward positive bias. After removing the negative bias, the recovery of trapped electrons can be observed and the device threshold voltage comes back to the original value. Until now, the micro process of electron trap generation under the positive bias stress is not discussed in detail.

The reversible positive ΔV_{th} not only caused by positive bias stress but also can be induced by H_2O and O_2 in ambient air. When there are lots of OH groups on the SiO_2 surface, SiOH is generated. H_2O and O_2 are easily absorbed by SiOH to cause electron traps at the pentacene/dielectric interface. This generation process can be shown as chemical reaction:



and



We can see H_2O and O_2 contained in air promote the reaction to the right-hand side and produce negative-charged states that cause the ΔV_{th} . Therefore, if we perform the measure in vacuum or eliminating OH groups on the dielectric surface, the prolonged positive bias influence on device V_{th} may be drastically reduced.

1.3.2 Resources of trapped carrier

Besides how defects form in OTFTs and cause ΔV_{th} , another question is where the charges that be trapped in these defects come from? Two resources had been suggested: carrier injection from electrode and photogenerated carriers. Carrier injection proposes that when gate is given bias stress, extra carrier can inject from electrode into organic semiconductor and accumulate. But with the pentacene-based OTFTs be used in this experiment, there is a high energy barrier at the junction

between Au electrode and LUMO of pentacene to block the electron injecting from electrodes. Therefore, the possibility that electron can inject from electrode is rare. The other resource is photogenerated carriers, When OTFTs is under illumination, the proper light intensity can induced excitons in the pentacene film. These photo-induced excitons then disassociate by gate bias into electrons and holes, which can be trapped by defects.

1.3.3 Field-Effect Mobility Degradation

Mobility degradation is also caused by defects. These defects can originally exist (i) in the semiconductor or grain boundary, defects can also generate by (ii) giving bias stress, (iii) absorbing H₂O and O₂ in the air. Mobility degradation is usually permanent damage while ΔV_{th} is often reversible, this means defects cause mobility degradation are in deeper state, trapped carriers are difficult to get out from these states.

Optimize the semiconductor deposition temperature, deposit rate, film thickness...etc, may diminish defects originally exist in active layer. On the other hand, passivation layer is usually used to protect organic semiconductor from H₂O and O₂ after OTFTs are fabricated. In short, prevent defects from forming is the best method to postpone mobility degradation.

1.4 Surface Treatment

The growth process of pentacene thin film can be described by diffusion limited aggregation. When initially growing pentacene thin film, molecules were vaped to the gate dielectric surface. Before meeting critical nuclei, molecules drifted on the surface. It is as well known that pentacene consists of thin film phase and bulk phase. Therefore, surface states of the gate dielectric greatly affect the pentacene growth.

When most components of pentacene film are thin film phase, pentacene-based TFTs have the best electrical performance.

There are many surface treatments proposed to improve the surface states of gate dielectric. Fundamental functions of using surface treatments are: (i) lowering leakage current, (ii) reducing surface trap states to enhance the field-effect mobility (iii) improving the device stability in ambient air and (ix) obtaining better device sense ability.

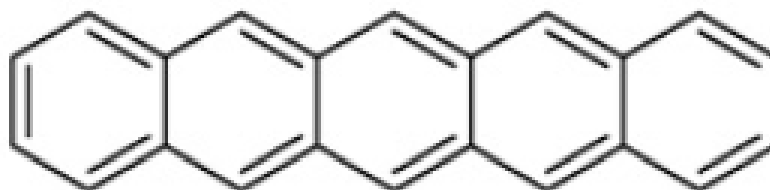
1.5 Motivation

Defects can induce the threshold voltage shift and mobility degradation. This leads Short lift time of OTFTs, and prohibit OTFTs from further application. We want to find out defects forming mechanism, and study how these defects react in different environment (ex. in dark/light, in air/vacuum)

PVP (with OH groups) and PMMA (without OH groups) were used as surface treating materials, bias stress measurement was taken in air/vacuum helping to know how H₂O and O₂ effect OTFTs operation. In order to observe how light effects OTFTs, measurement was also taken in dark, under light, illuminate with different wavelength light.

Combine above bias stress measurement results and material analysis. We hope this experiment can help us better understand how carriers be trapped and make some contribution to realize OTFTs application.

Figure of Chapter 1



Pentacene

Fig. 1. 1 Pentacene molecular structure

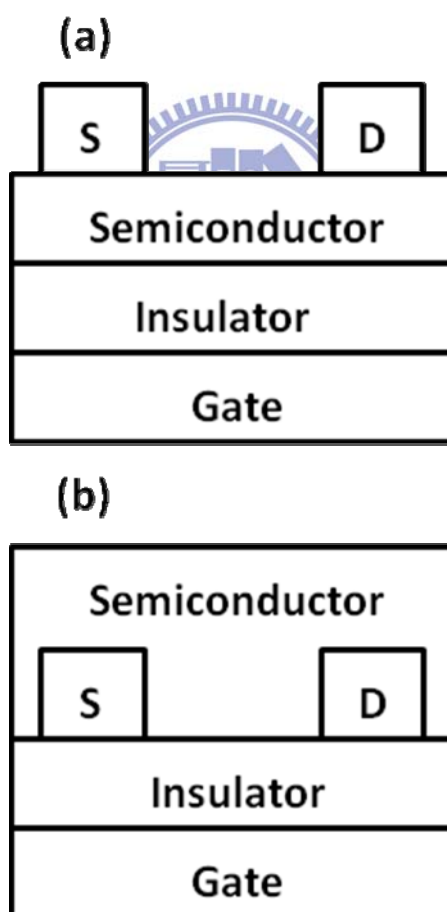


Fig. 1. 2 OTFT device configurations. (a) cross section view of top contact device. (b) cross section view of bottom contact device.

Chapter 2

EXPERIMENTAL SETUP

2.1 Device Fabrication

In this study, conventional top-contact pentacene-based TFTs with dual dielectric layers were used. 100-nm-thick thermal oxide was grown on heavily doped Si wafers to serve as the first layer of gate dielectric. The back of heavily doped Si wafer is served as the gate electrode. Poly (methyl methacrylate) (PMMA) and PVP (poly-4-vinyl phenol) were separately used as second dielectric layers to provide different surface states.

Device Fabrication Process Flow:

Step1. Clean the oxide surface



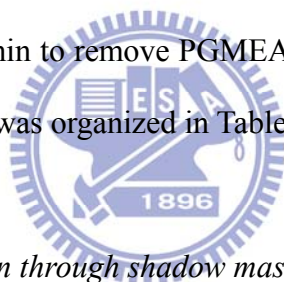
Before fabricating device on wafer, the native oxide on the back of wafer must be etched by using BOE ($\text{NH}_4\text{F} : \text{HF} = 10 : 1$) solution. Then, the oxide surface of wafer was cleaned by 5 mins DI water, 5 mins acetone and 5 mins DI water, sequentially. Using hot plate bakes the wafer to remove the moisture on the oxide surface.

Step2. Organic dielectric layer fabrication

PMMA fabrication condition: PMMA was obtained from MicroChem. Corp. with molecular weight of 95000 and was dissolved in anisole at 10 wt%. Fig. 2.1 is the molecular structure of PMMA. The spin speed was accelerated from 0 to 1000 rpm during the first 10 sec and further increased the spin speed from 1000 rpm to

6000 rpm in following 10 sec. After keeping 6000 rpm of the spin speed for 40 sec, the spin speed was decreased from 6000 rpm to 0 rpm in following 10 sec. Then, using hot plate baked the sample for 30 mins at 70°C.

PVP fabrication condition: PVP was obtained from Aldrich with molecular weight about 20000. PVP have OH function groups on its molecule structure as shown in Fig. 2.2, poly (melamine-co-formaldehyde) MMF was used as cross-linker and dissolved in PGMEA (propylene glycol 1-monomethyl ether 2-acetate, C₆H₁₂O₃). Fig. 2.3 is schematic picture of MMF cross-link with PVP. Most of PVP spin conditions were similar to above PMMA fabrication process except the initial acceleration from 0 to 1000 rpm was finished in 5 seconds. Then, PVP was cross-linked by thermal curing through a hot plate in air. At temperatures of 100 °C for 10 min and 200 °C for 50 min to remove PGMEA in the PVP film [1-3]. The spin conditions of PMMA and PVP was organized in Table 2.1



Step3. Pentacene film deposition through shadow mask

Pentacene obtained from Aldrich (purity: 99.9%) without purification was evaporated through a shadow mask onto thermal oxide to form the active layer. The deposition rate was set at 0.5 Å/s. The substrate temperature and the pressure were kept at room temperature and at around 3×10^{-6} Torr during deposition process.

Step4. Depositing Au to form source and drain contact

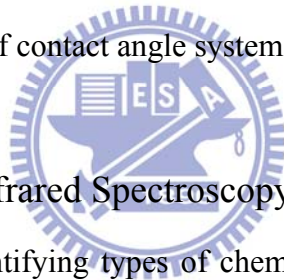
After depositing a 100-nm-thick pentacene, 100-nm-thick gold was deposited through the shadow mask to form source/drain contacts. The thickness of Au layer was 100 nm. The device channel length varied from 100 μm to 600 μm while channel width was fixed as 1000 μm.

The structure scheme of pentacene-based TFTs with PMMA or PVP dielectric layers are shown in Fig. 2.4.

2.2 Material Analysis Instrument

2.2.1 Contact angle system

Contact angle system is used to estimate wetting ability of a localized region on a solid surface. The angle between the baseline of the drop and drop boundary is measured. Comparing the result can tell the material surface is relatively hydrophile or hydrophobic, then can further analysis surface chemical composition. Since PVP have OH groups on its molecular structure while PMMA do not have, PVP surface should be more hydrophile and have smaller contact angle compare with PMMA surface. Fig. 2.5 is the picture of contact angle system used in this experiment.



2.2.2 Fourier Transform Infrared Spectroscopy (FTIR)

FTIR is powerful tool for identifying types of chemical bonds (function groups) in organic molecular. The wavelength of light absorbed is characteristic of the chemical bond, by analyzing the infrared absorption spectrum, the chemical bonds in a molecule can be determined. In this experiment, OH groups' absorption spectrum can be find in library of known compounds, using FTIR is the more accurate method to check if PVP surface have OH groups. Fig. 2.6 shows some common function groups' absorption spectrum.

2.2.3 X-Ray Diffraction (XRD)

X-ray diffraction (XRD) is a non-destructive technique that reveals detailed information about the chemical composition and crystal structure of materials. The crystal lattice is a regular three-dimensional distribution of atoms in space. Atoms are arranged and form a series of parallel planes separated from one another by a distance d , which varies according to the nature of the material. When monochromatic X-ray project onto a crystalline material at particular angle (Θ), diffraction will occurs because the ray traveled distances reflected from successive planes differs by a complete number n of wavelength. Plotting the angular positions and intensities of the diffracted peaks produces a pattern, which is characteristic of the sample. In this experiment, XRD is used to check two things. First is to find if pentacene is successfully deposited on PMMA and PVP surface, this can be told by diffracted peaks exists at certain angles. Second is to know the crystallization of pentacene grow on PMMA and PVP, this can be told by pentacene peaks intensity. Fig. 2.7 is the picture of Shimadzu XRD-6000.

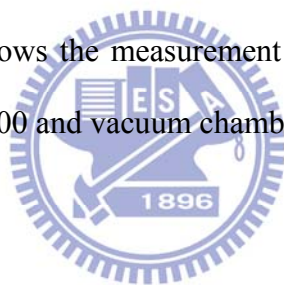
2.2.4 Atomic force microscope (AFM)

Since PVP treated surface may exist OH groups, its surface morphology can also be different compare with PMMA surface. In addition, pentacene deposits on PVP (hydrophile) and PMMA (hydrophobic) influenced by these two kinds of surfaces may have different grain size or morphology, too. Atomic force microscope (AFM) is used to measure surface morphology on a scale from angstroms to 30 microns. It scans samples through a probe or tip, with radius about 20 nm. The tip is held several nanometers above the surface and using feedback mechanism that measured interactions between tip and surface on the scale of nanoNewtons. Variations in tip height are recorded when the tip is scanned repeatedly across the sample, then

producing morphology image of the surface. In this experiment, the used equipment is Digital Instruments D3100 as shown in Fig. 2.8 and the used active mode is tapping mode.

2.3 Device Electrical Characteristic Measurement

Two measurement systems were used in this study. In ambient air condition, using semiconductor parameter analyzers HP4156 or Keithley 5270 measured devices in metal box at room temperature. Another measurement system includes semiconductor parameter analyzer Keithley 4200 and vacuum chamber. The chamber pump can lower the pressure in chamber from 760 Torr to 0.5 Torr. Therefore, measurements can be performed in vacuum at room temperature to compare H₂O and O₂ influences on device stability. Fig. 2.9 shows the measurement system includes semiconductor parameter analyzer Keithley 4200 and vacuum chamber.



2.4 Illumination Setup

There are four different light sources to illuminate the device in this experiment. The white light source comes from light-emitting diode (LED) backlight with a broad wavelength range. Blue, green and red light sources are light-emitting diodes with 467 nm, 536 and 631 nm wavelengths. These spectrums of four light sources are shown in Fig. 2.10. The light source was set up above the device to irradiate the sample from the top. The light power was controlled by the power supply (PPT3615). The light intensity was adjusted by changing the applied voltage.

2.5 Device Electrical Parameters Extraction

Field effect mobility, threshold voltage, subthreshold slope and I_{on}/I_{off} ratio are usual used to compare different devices' performance. In the following section, extraction methods would present how to extract parameters from electrical transfer characteristic of pentacene.

2.5.1 Field Effect Mobility

The field effect mobility (μ_{FE}) was determined by the orientation of pentacene molecules near gate dielectric. Therefore, gate dielectric surface states strongly affect the device μ_{FE} . The device μ_{FE} variation can be used to compare the difference between PMMA and PVP dielectric layers. In our experiment, μ_{FE} were extracted by using the linear region equation. Because the electrical transfer characteristic of pentacene-based thin film transistor is similar to those conventional single crystalline MOSFETs, the linear region equation can be applied to pentacene-based thin film transistor and can be expressed as

$$I_{DS} = C_{eff} \mu_{FE} \frac{W}{L} \left[(V_{GS} - V_{th}) V_{DS} - \frac{1}{2} V_{DS}^2 \right]$$

where C_{eff} and V_{th} are effective capacitance per unit area and the threshold voltage. W and L are device channel width and channel length. When operating device at low drain bias, the linear region equation can be modified to

$$I_{DS} = C_{eff} \mu_{FE} \frac{W}{L} (V_{GS} - V_{th}) V_{DS}$$

After differentiating Eq.(*) with respect to $(V_G - V_{th})$, the device transconductance can

be written as $G_M = C_{eff} \mu_{FE} \frac{W}{L} V_{DS}$

The field effect mobility can be extracted from the transconductance and this equation

can be expressed as $\mu_{FE} = \frac{L}{W V_{DS} C_{eff}} G_M$

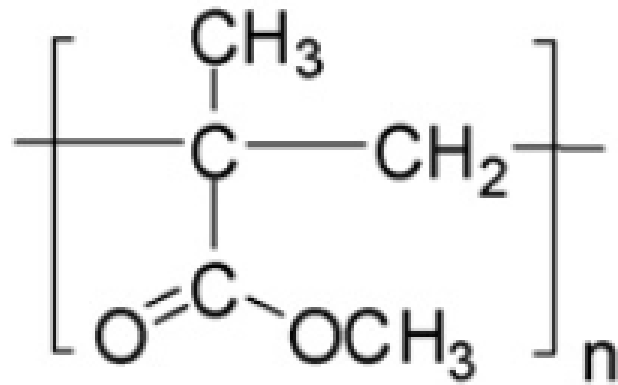
In this study, we used max G_M value to calculate and define the field effect mobility.

2.5.2 Threshold voltage

Threshold voltage (V_{th}) determines the device operation voltage and smaller V_{th} can help to lower power consumption. Because V_{th} strongly depends on dielectric surface states, environmental and fabrication process variations easily cause a shift on the V_{th} . Based on this phenomenon, the device V_{th} shift is usually used as an importance parameter when pentacene-based TFTs applied to Photo detector or Chem-Bio detector. In this study, we used the linear region equation to extract the device V_{th} .

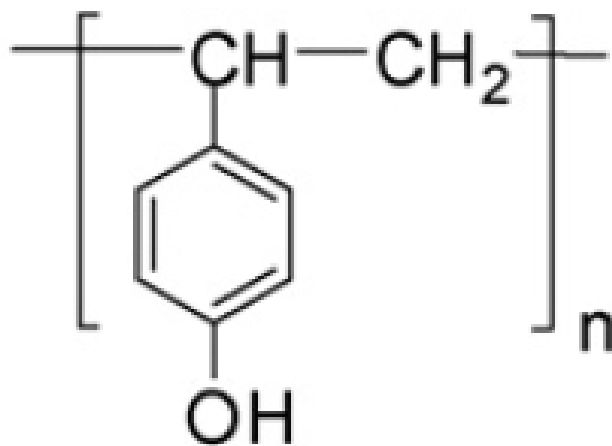


Figure of Chapter 2



PMMA

Fig. 2.1 PMMA molecular structure



PVP

Fig. 2.2 PVP molecular structure

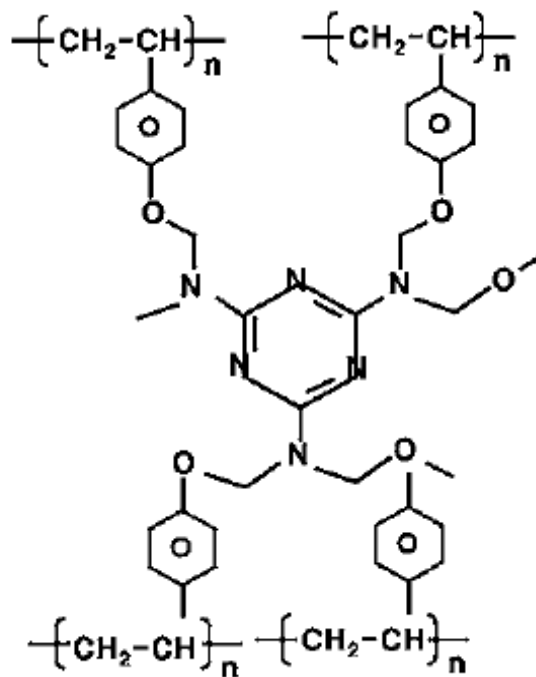


Fig. 2. 3 Schematic picture of MMF cross-link with PVP

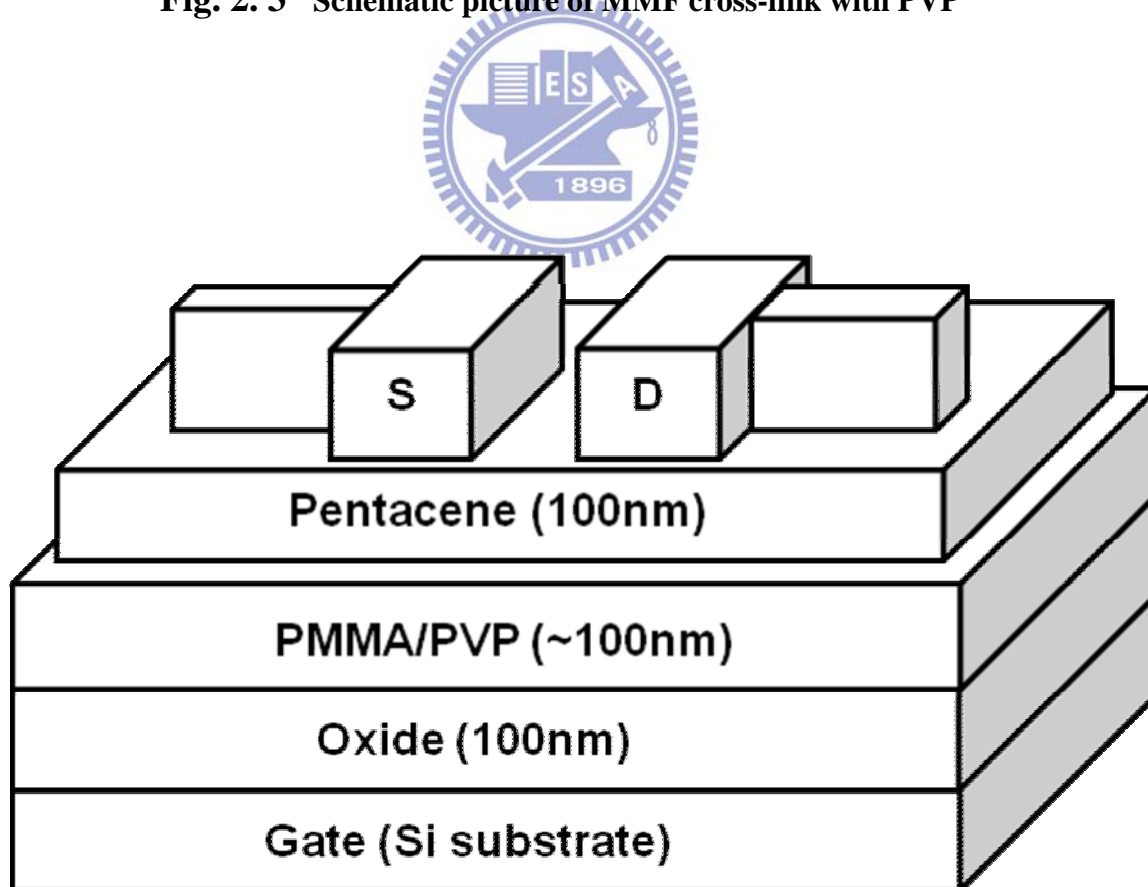


Fig. 2. 4 Schematic structure of PVP-OTFTs and PMMA-OTFTs

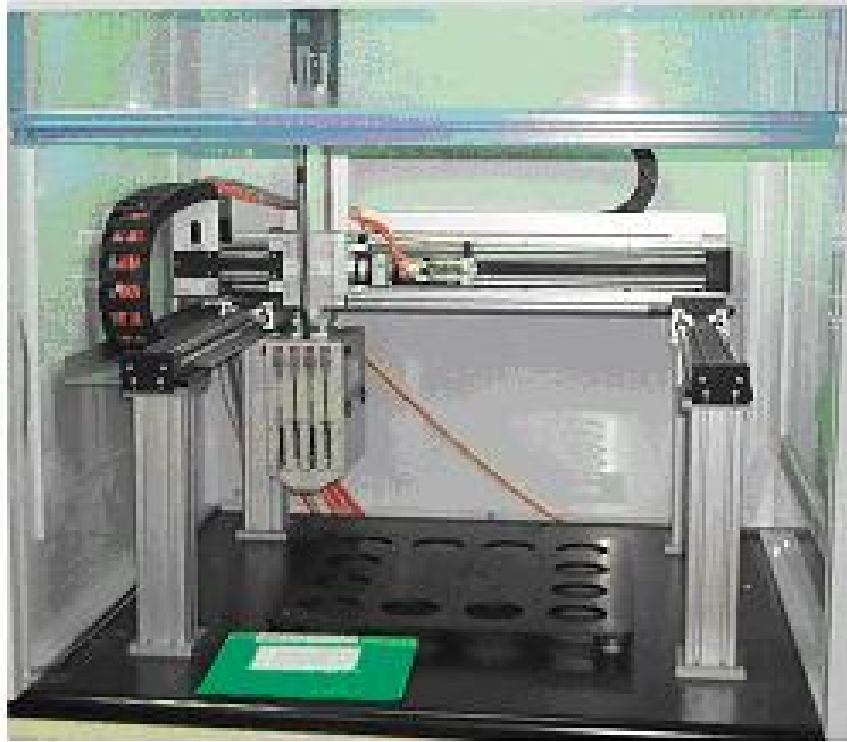


Fig. 2. 5 image of contact angle system

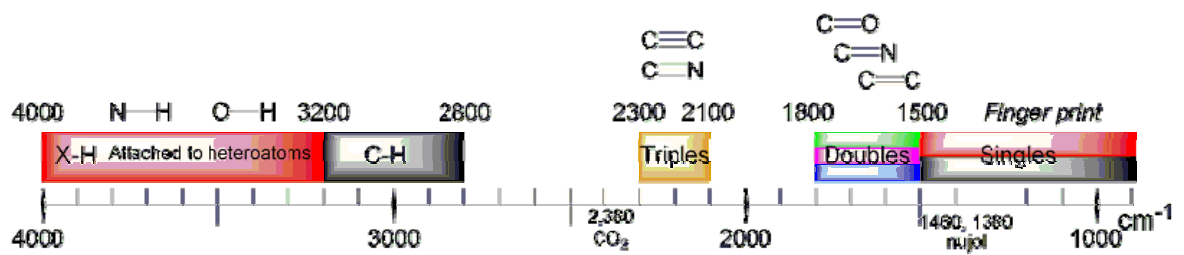


Fig. 2. 6 Absorbance spectrum of different function groups



Fig. 2. 7 Picture of Shimadzu XRD-6000

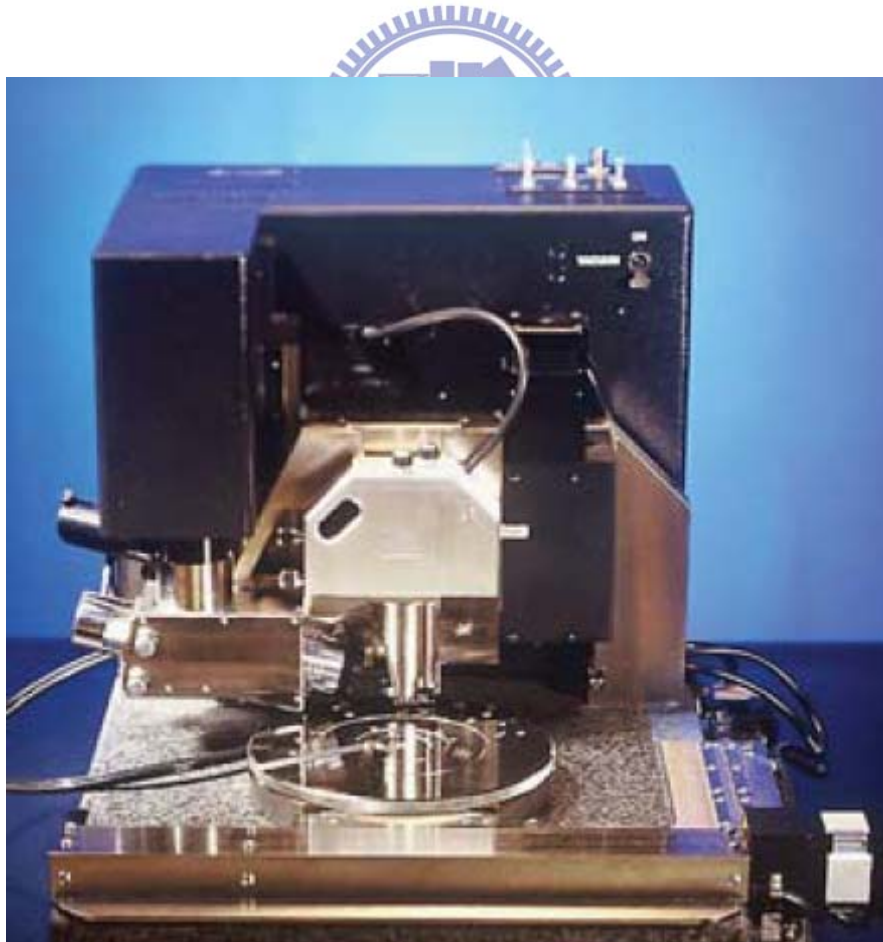


Fig. 2. 8 Picture of Digital Instruments D3100

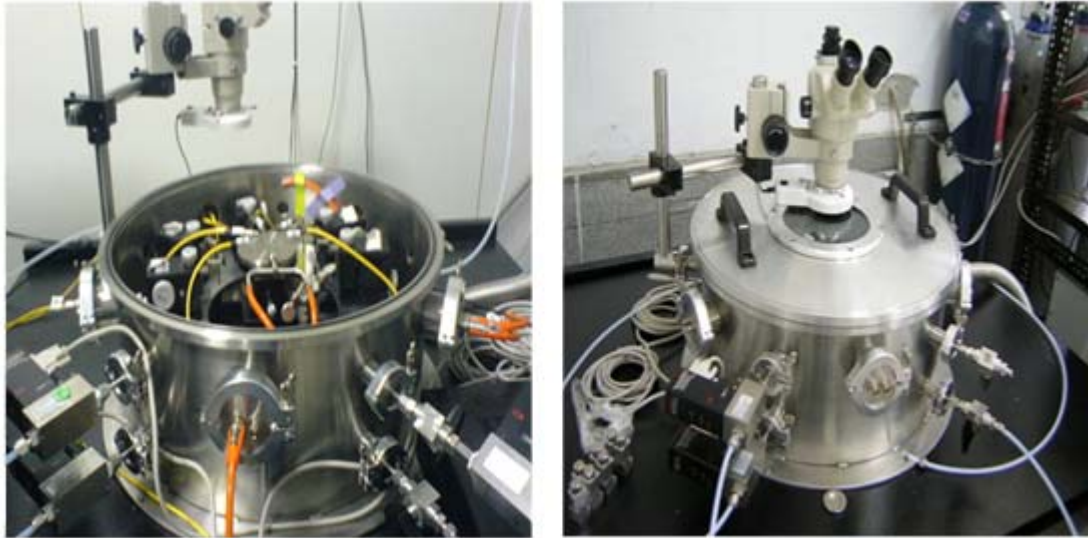


Fig. 2. 9 Picture of vacuum chamber



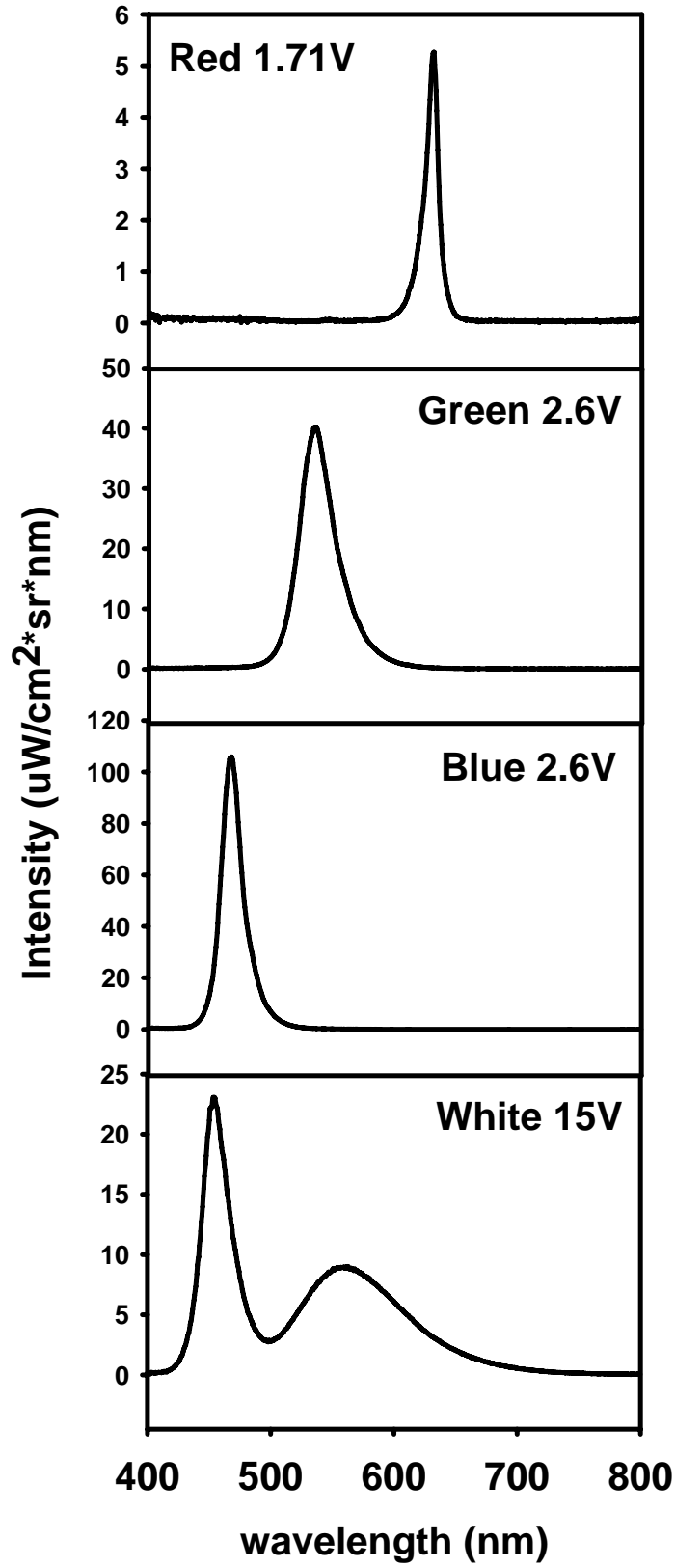


Fig. 2. 10 Intensity of LED (Red, Green ,Blue and White) wavelength spectrum

Table of Chapter 2

| PMMA | Time (second) | spin speed (rpm) |
|-------------|----------------------|-------------------------|
| | 0 ~ 10 | 0 |
| | 10 ~ 20 | 0 ~ 1000 |
| | 20 ~ 30 | 1000 ~ 6000 |
| | 30 ~ 70 | 6000 |
| | 70 ~ 80 | 6000 ~ 0 |
| PVP | Time (second) | spin speed (rpm) |
| | 0 ~ 10 | 0 |
| | 10 ~ 15 | 0 ~ 1000 |
| | 15 ~ 25 | 1000 ~ 6000 |
| | 25 ~ 65 | 6000 |
| | 65 ~ 75 | 6000 ~ 0 |

Table 2.1 PMMA and PVP spin coating parameters

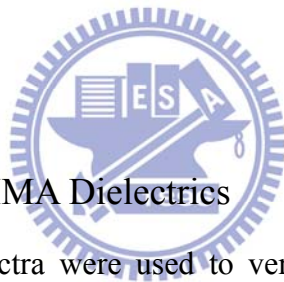
Chapter 3

Analysis and Results

3.1 Material Analysis of PVP and PMMA

3.1.1 Wettability of PVP and PMMA Dielectrics

PMMA and PVP were fabricated by using spin-coating process on silicon wafer. Contact angles of PMMA and PVP dielectric surfaces were 61.7° and 51.8° as shown in Fig. 3.1. Previous researches mentioned that the moisture contact angle strongly depends on the chemical composition of dielectric surface [11]. Fig. 3.1 shows that PVP dielectric surface is more hydrophilic than PMMA because OH groups exist in PVP molecule structure.



3.1.2 FTIR of PVP and PMMA Dielectrics

The FTIR absorption spectra were used to verify OH groups exist in PVP dielectric surface. The FTIR absorption spectra of PVP and PMMA dielectric layers were shown in Fig. 3.2. For PVP absorption curve, there are two stretching bands at 3355 cm^{-1} and 3000 cm^{-1} , which were attributed to the OH groups and C–H groups, respectively [12-13]. However, there is no obvious stretching band at 3355 cm^{-1} in PMMA absorption curve. This result shows that OH groups do not exist in PMMA dielectric surface.

3.2 Electric Transfer Characteristics of Devices with PVP and PMMA

Dielectrics

Based on above results, pentacene thin films were deposited on organic dielectric with and without OH groups to form thin film transistors. Electrical transfer characteristics of pentacene-based TFTs with PVP and PMMA dielectrics were shown in Fig. 3.3. Subthreshold swing and on/off ratio of PVP-OTFTs are similar to PMMA-OTFTs. The threshold voltage of PVP-OTFTs and PMMA-OTFTs were about -3 ~ -6 V and -14 V. The field effect mobility of PVP-OTFTs and PMMA-OTFTs were about $0.6 \text{ cm}^2/\text{V}\cdot\text{s}$ and $0.36 \text{ cm}^2/\text{V}\cdot\text{s}$. In our experiment, the field effect mobility of PVP-OTFTs was larger than PMMA-OTFTs.

It had been reported that the device mobility was affected by the pentacene grain size [14-16]. Some groups proposed that the larger grain size help to enlarge the device mobility. If pentacene grain size is small, there are many grain boundaries in the device channel which include many trap sites to block the free carrier transportation.

However, other groups found the opposite result [5] and they thought that the device mobility was mainly dominated by pentacene growth mode. If Stranski - Krastanov growth mode (two dimensional growth mode) is observed at the beginning of pentacene deposition, the molecules near substrate will strongly bind to substrate than bind with other molecules. This kind of growth mode will leave lots of voids in the first layer of pentacene and cause lower carrier mobility. In contrast, if Volmer-Weber growth mode (three dimensional growth mode) is observed, pentacene molecule will highly interconnect with one another and have less voids, the mobility then become higher.

Although many superior groups tried to clarify the relationship between pentacene grain size and device mobility, the grain size is still difficult to use to

estimate the device mobility. Therefore, in following section, the morphology and phase composition of the pentacene films grown on PVP and PMMA gate dielectrics which greatly influence the device performance will be discussed in detail.

3.2.1 XRD Analysis of PVP and PMMA Dielectrics

Using x-ray diffraction (XRD) studied the structural order difference between pentacene films grown on PVP and PMMA dielectrics. XRD pattern of the pentacene film consist of the thin-film phase and the single-crystal (bulk) phase [17]. Thin-film phase is defined when reflection plane spaces (d_{001}) are 15.66 Å, 7.78 Å, and 5.17 Å ($l = 1, 2,$ and $3,$ respectively). It is usually found in vapor deposited thin film and is kinetically favored phase. On the other hand, single-crystal phase is observed when reflection plane space (d_{001}) is 14.61 Å, 7.26 Å, and 4.82 Å ($l = 1, 2,$ and $3,$ respectively), single-crystal phase is thermodynamically stable phase. Fig. 3.4 shows that XRD patterns of 100nm-thick pentacene films deposited on PVP and PMMA gate dielectrics. Both PVP and PMMA samples have series of (d_{001}) reflections which shows the formation of “thin-film” phase. Next we can find both two samples have obvious peak fractions from (d_{001}) to (d_{003}) in the XRD pattern. These features suggest that molecules in the pentacene film are well-oriented perpendicular to the dielectric interface [18].

3.2.2 Morphology of PMMA, PVP and Pentacene Films

Before and after depositing pentacene thin film on organic gate dielectric, using atomic force microscope (AFM) observes the morphology of PMMA, PVP and pentacene films. Surface roughness is one of factors that can effect semiconductor crystallization. Pentacene grow on smooth surface usually have better morphology and mobility than grow on rough surface. Fig. 3.5(a) and (b) are atomic microscopy images of PMMA and PVP gate dielectrics before depositing pentacene thin films. Both PMMA and PVP have smooth surface roughness about 0.3 nm. Fig. 3.5 (c) and (d) are atomic microscopy images of 25 Å pentacene thin films on PMMA and PVP gate dielectrics. By telling (c) and (d) images, pentacene grow on PVP surface have bigger grain size than pentacene grow on PMMA surface. It may be the reason why PVP-OTFTs have larger mobility[19].



3.2.3 Hysteresis

Hysteresis was widely observed in the transfer characteristic of pentacene-based TFTs and used to explain the dielectric interface states. Devices with PMMA and PVP dielectrics were prepared to measure by semiconductor parameter analyzers HP4156. First, measurements were performed in ambient air and in dark. Gate bias region of transfer characteristics for devices with PMMA and PVP dielectrics is differing. Because the threshold voltage of device with PVP dielectric is smaller than with PMMA dielectric, we extended gate bias in positive region from 10 V to 15 V. Fig.3.6 (a) and Fig.3.7 (a) are electrical transfer characteristics of devices with PMMA and PVP dielectrics swept in both directions (on to off and off to on). For devices with PMMA and PVP dielectrics, hysteresis was not observed in dark environment. When measurements were performed in ambient air under illumination, hysteresis was only observed in device with PVP dielectric as shown in Fig.3.6 (b)

and Fig.3.7 (b). The light power was kept at 16.9 mW/cm^2 during measuring device. Device with PVP dielectric had significant hysteresis by shifting the threshold voltage from -6.23 V to -1.28 V .

In previous studies, it was proposed that organic dielectric itself was a main issue to cause hysteresis. The gate electrical field maybe reorients dipolar groups in the organic dielectric. The origins of the dipoles may be residual hydroxyl OH groups due to incomplete cross-linking residual, OH groups from the solvent due to incomplete baking after film formation or adsorbed water molecules due to exposure to ambient air [20-22]. However, hysteresis in transfer characteristics for devices with PMMA and PVP dielectrics were not observed when measured in dark. Therefore, OH groups in PVP dielectric was not affected and reoriented by gate electrical field. In previous reports, Gu et al. proposed that trapped electrons in the semiconductor have very long lifetimes. It was found that time constants of electron detrapping was the order of second or more. Therefore, trapped electrons can not be released in time and stored in the semiconductor to induce extra drain current. The illumination and the ambient air also dominated the hysteresis in transfer characteristic [23-25].

In our experiment, it was found that dielectric interface needed OH groups to cause hysteresis even if device was measured in ambient air under illumination compare with Fig.3.6 (b) and Fig.3.7 (b).

3.3 Bias Stress and Hydroxyl Groups Influence on the Device Threshold Voltage

As above description, pentacene thin film deposited on organic dielectrics with and without OH groups had different interface states between gate dielectric and pentacene thin film [26-27]. In this section, we discuss the OH group influence on the device reliability, the photodetectability and the defect generation mechanism. In

previous researches, they proposed that increasing OH groups at the interface can enhance the device photoresponsivity. However, one of main degradation mechanisms is OH group existence at the interface and pentacene thin film. In our previous study, it was found that adjusting the electrical field can control the photoresponsivity of pentacene -based TFTs. Therefore, combining bias stress and illumination was applied to devices with different interface states to discuss carrier generation and transport mechanisms and the defect generation mechanism.

3.3.1 Bias Stress in Dark Environment

In initial study, the bias stress effect on devices with and without OH groups at dark and ambient air environment was discussed. Because Au/pentacene contact barrier is prefer to hole transport, pentacene-based TFTs in this study is p-type. The positive gate bias was applied to stress the device at off-state region and the negative gate bias was applied to stress the device at on-state region.

For positive gate-bias stress, V_G was kept at 15 V and $V_D = V_S$ were 0 V for 1000 sec. The linear-region transfer characteristics of devices before stress and after 1000-sec stress are depicted in Fig.3.8. Then, threshold voltage shift (ΔV_{th}) curves of devices with PMMA and PVP gate dielectrics were plotted as a function of bias stress time as shown in Fig. 3.9. We found that positive gate-bias stress influences on devices with PMMA and PVP gate dielectrics were differing. The electrical transfer characteristic of device with PMMA gate dielectric is near unchanged. Obviously the gate-bias stress causes a shift of the transfer characteristics of device with PVP gate dielectric while the subthreshold swing keeps almost unchanged. The field-effect mobility μ_{FE} as a function of stress time is shown in Fig. 3.10. μ_{FE} is not affected by the stress, while V_{th} is drastically changed.

For the negative gate-bias stress, V_G was kept at $-15+V_{th}$ V while $V_D = V_S$ were 0

V for 1000 sec. The linear-region transfer characteristics of devices before stress and after 1000-sec stress are depicted in Fig. 3.11. Then, threshold voltage shift (ΔV_{th}) curves of devices with PMMA and PVP gate dielectrics were plotted as a function of bias stress time as shown in Fig. 3.12. The negative bias stress caused a ΔV_{th} of both transfer characteristics of device with PMMA and PVP gate dielectrics while their subthreshold swing kept almost unchanged. The ΔV_{th} of device with PVP gate dielectric is larger than with PMMA gate dielectric. Compare to the positive gate bias stress, the negative gate bias stress caused the obvious ΔV_{th} of device with PMMA dielectric but it was smaller than the ΔV_{th} of device with PVP dielectric. The field-effect mobility μ_{FE} as a function of stress time is shown in Fig. 3.13, μ_{FE} is not affected by the stress.

Under the positive bias stress experiment, extra energy is given to help forming acceptor-like traps (electron traps) to grabbing electrons. PMMA-OTFTs (without OH groups) are excellent stable while PVP-OTFTs (with OH group) have distinguishable ΔV_{th} in positive stress condition further confirm that OH groups on the interface tend to form traps and grab electrons.

Next, we take a look into negative bias stress experiment. When prolonged negative gate voltage is applied, holes will accumulate in channels. These holes are then trapped in deep energy states located within the pentacene molecules near the dielectric interface, or are trapped at the defect states of pentacene grain boundaries near the interface. The trapped holes screen the gate field, which in turn cause the negative shift of the threshold voltage [28]. Because the pentacene deposit on PVP and PMMA devices have this donator-like (hole traps) defects, so both of two kinds of devices had negative ΔV_{th} . Pentacene grow on PVP have more defects. So under negative gate bias stress, PVP-OTFTs will have more negative ΔV_{th} .

3.3.2 Bias Stress under Illumination

When devices were operated under illumination, many researches found that the device threshold voltage shifted forward the positive voltage. The light-induced ΔV_{th} was attributed to light-induced carriers in the channel and dependent on carrier concentration. In our previous study, the light-induced carrier concentration can be controlled by the drain bias while illuminating the devices.

In this experiment, the light power was setup at 2.95 mW/cm^2 and 1000-sec applied gate bias. Transfer characteristics of devices with PMMA and PVP dielectrics were measured in ambient air. First, the illumination influence on the device threshold voltage without the gate bias was studied. After 1000-sec illumination on devices with PMMA and PVP dielectrics, the ΔV_{th} of device with PVP dielectric shifted forward positive and was larger than with PMMA dielectric as shown in Fig. 3.14. Although the illumination influence on the device threshold voltage is slight, it was found that OH groups at the insulator interface can enhance the light-induced ΔV_{th} .

In following experiments, devices with PMMA and PVP dielectrics were stressed under illumination. The gate bias was setup at 15 V and $V_D = V_S$ were 0 V and devices were measured in ambient air. The linear-region transfer characteristics of devices before stress and after 1000-sec stress are depicted in Fig. 3.15. Then, threshold voltage shift (ΔV_{th}) curves of devices with and without illumination were plotted as a function of bias stress time as shown in Fig. 3.16. Compared to results of section 3.3.1, the ΔV_{th} of device with PMMA dielectrics is significantly enhanced by illumination and the device ΔV_{th} increment is larger than with PVP dielectrics. Although the ΔV_{th} increment of the device with PVP dielectrics is slight, the illumination accelerates the device ΔV_{th} reaching the saturation value.

It is plausible that the electrical field helps to dissociate light-induced excitons to hole-electron pairs and light-induced electrons were accumulated in the channel by

the positive gate bias. The light-induced ΔV_{th} is proposed to be limited by the applied gate bias. A band diagram from gate to drain is used to explain the proposed mechanism [29-31]. As shown in Fig. 3.17, when a positive gate bias is applied, the lowered Fermi energy (E_F) in the gate electrode leads to a downward band bending of pentacene near the gate dielectric. The band bending provides more trap sites in the forbidden gap to capture light-induced electrons. Therefore, when total trap sites provided by band bending are filled, the light-induced ΔV_{th} reaches saturation.

However, for the device with PMMA dielectric, the obvious ΔV_{th} increment caused by combining gate bias stress and illumination was waited for solved. Some previous studies also mentioned that applying positive gate bias to stress pentacene-based TFTs only caused the slight ΔV_{th} if the environment is dark. The pentacene-based thin film transistor is p-type due to Au/pentacene contact. Because the Fermi level of Au contact is near the LOMO (lowest unoccupied molecule orbital) of pentacene film, electrons are difficult to inject into the pentacene film from Au contact. Therefore, the positive gate bias can not accumulate electrons in the channel near the dielectric due to Au/pentacene contact. If illuminating the device under bias stress, light-induced excitons and electrical field will provide electrons to accumulate at channel near gate dielectric and cause the device ΔV_{th} . However, after stressing at dark, the ΔV_{th} of device with PVP dielectric is obvious. This difference between devices with PMMA and PVP dielectrics maybe is caused by different defect generation mechanisms.

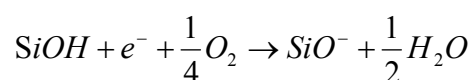
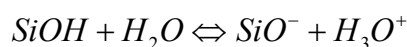
For the device with PVP dielectric, there are many OH groups at dielectric surface. Therefore, two plausible mechanisms were proposed. 1. Thermal generation: OH groups between dielectric and pentacene film form a lot of carrier generation center to generate hole-electron pairs. 2. Moisture influence: OH groups between dielectric and pentacene film capture moisture to generate negative defects [32-36].

When extending gate bias stress time, the ΔV_{th} of device with PVP dielectric under illumination reached a larger saturation value than under dark, as shown in Fig. 3.18. The increment between ΔV_{th} curves stressed by gate bias with and without illumination is difficult to explain by the thermal generation mechanism. In previous discussion on energy band of pentacene film, the saturation value of device ΔV_{th} should be limited by the gate bias. Therefore, it represents that OH groups at dielectric surface and moisture in air contribute a lot defects to cause the device ΔV_{th} . In following experiment, devices were measured in vacuum to compare with that in air and discussed moisture influence on the defect generation mechanism.

3.3.3 Bias Stress in Vacuum Environment

This measurement system includes semiconductor parameter analyzer Keithley 4200 and vacuum chamber. The chamber pump can lower the pressure in chamber from 760 Torr to 0.5 Torr. Devices were measured in the chamber under dark. Then, threshold voltage shift (ΔV_{th}) curves of devices with PMMA and PVP gate dielectrics were plotted as a function of bias stress time as shown in Fig. 3.19. As expected, the threshold voltage of device with PMMA dielectric was near unchanged. Obviously, the ΔV_{th} of device with PVP dielectric was significantly suppressed while stressing the device at vacuum. Therefore, when stressing devices in air, generated defects can be attributed to the combination of moisture and OH groups

The previous study proposed that SiOH at the dielectric interface react with H₂O and O₂ in ambient air to cause the device ΔV_{th} forward positive bias [37]. The chemical react equation is shown in below.



In previous discussion, the saturant device ΔV_{th} was proposed to be dominated by the gate bias. If the proposed mechanism is correct, the ΔV_{th} of devices with PMMA and PVP dielectrics stressed by gate bias and illumination in vacuum should be the same. Fig. 3.20 shows that both ΔV_{th} of device with PMMA dielectric and with PVP dielectric are similar. Therefore, the larger saturant ΔV_{th} of device PVP dielectric stressed by gate bias and illumination in ambient air were simultaneously contributed by light-induced electrons and moisture-induced defects.

3.3.4 Different Light Wavelength Influence

Final, the relationship between different light wavelengths and the device ΔV_{th} was discussed. According to the study proposed by Yong-Young Noh et al [38], the influence of wavelength on the irradiation effect of pentacene-based OTFTs had been discussed. A smaller light-induced ΔV_{th} was found when the incident light had larger wavelength due to the internal filter effect. When illuminating the pentacene-based TFTs, the device threshold voltage shifted toward positive because that the light-induced electrons close to the gate dielectric were trapped by the interface states. If the wavelength had high absorption in pentacene, it was not able to arrive at the gate dielectric interface effectively.

In this experiment, red, green and blue light-emitting diodes (LEDs) were used as light sources to discuss light wavelength influence on the device ΔV_{th} . Fig. 3.21 shows that the device ΔV_{th} increased with decreasing light wavelength and the ΔV_{th} of device with PVP dielectric is larger than with PMMA dielectric. Based on the internal filter effect, the light-induced ΔV_{th} was dominated by light absorption spectrum. The light absorption spectrum of devices with PVP and PMMA dielectrics was shown in Fig. 3.22. Obviously, the light absorption spectrum was not affected by OH groups at gate dielectric interface. Therefore, curves with PMMA and PVP dielectrics were

parallel. For device with PVP dielectric, the ΔV_{th} increment was proposed to be contributed from moisture influence on the device ΔV_{th} .



Figure of Chapter 3

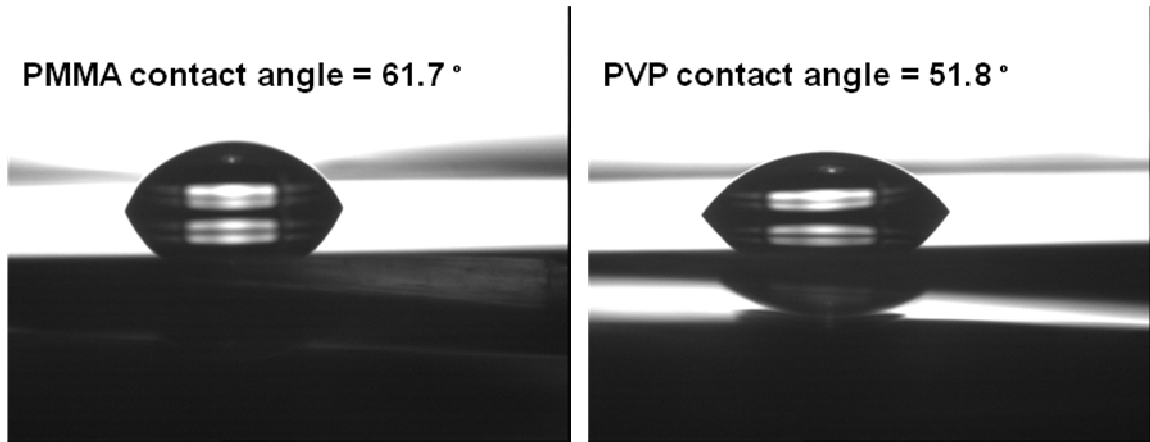


Fig. 3. 1 Moisture contact angle of PVP and PMMA dielectric

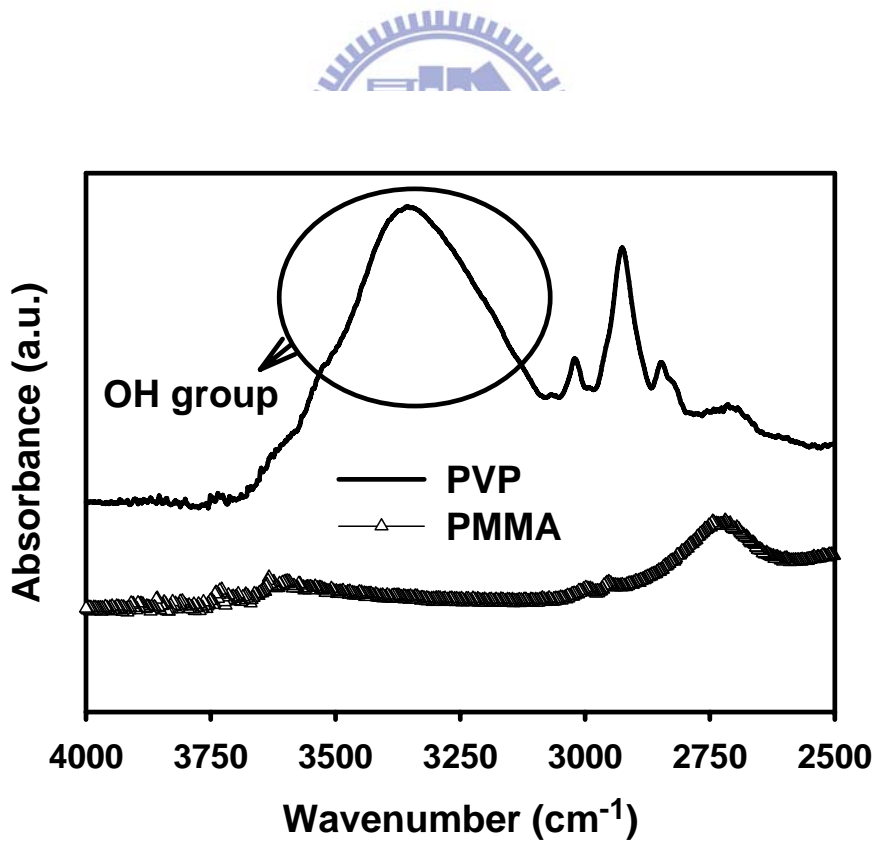


Fig. 3. 2 FTIR spectra of PVP and PMMA film.

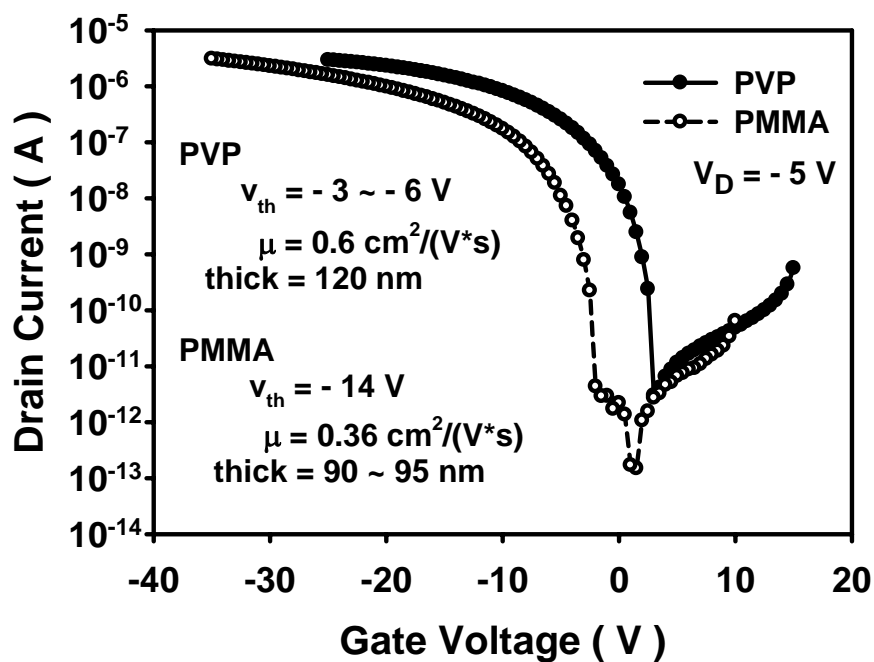


Fig. 3. 3 The initial transfer characteristic of PVP-OTFTs and PMMA-OTFTs

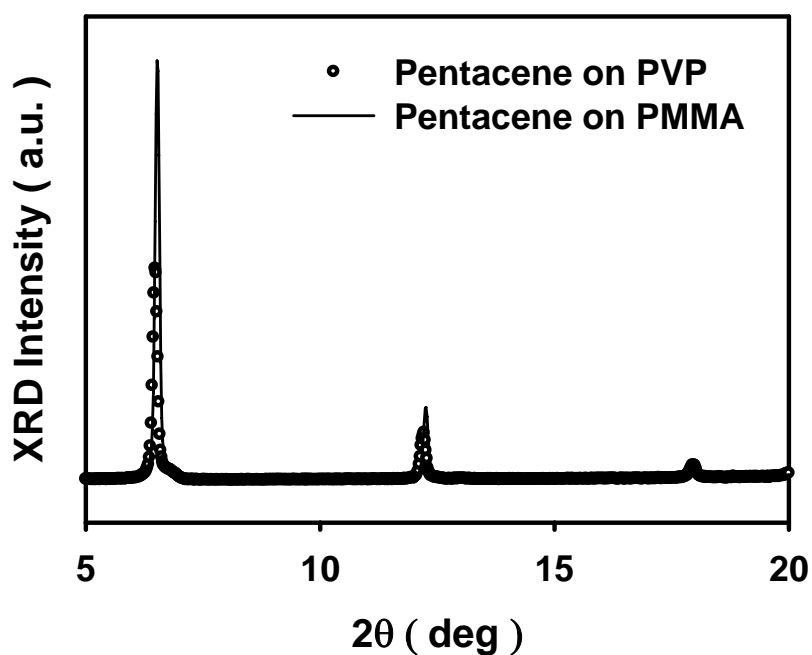


Fig. 3. 4 X-ray diffraction (XRD) pattern of pentacene deposit on PVP and PMMA dielectric

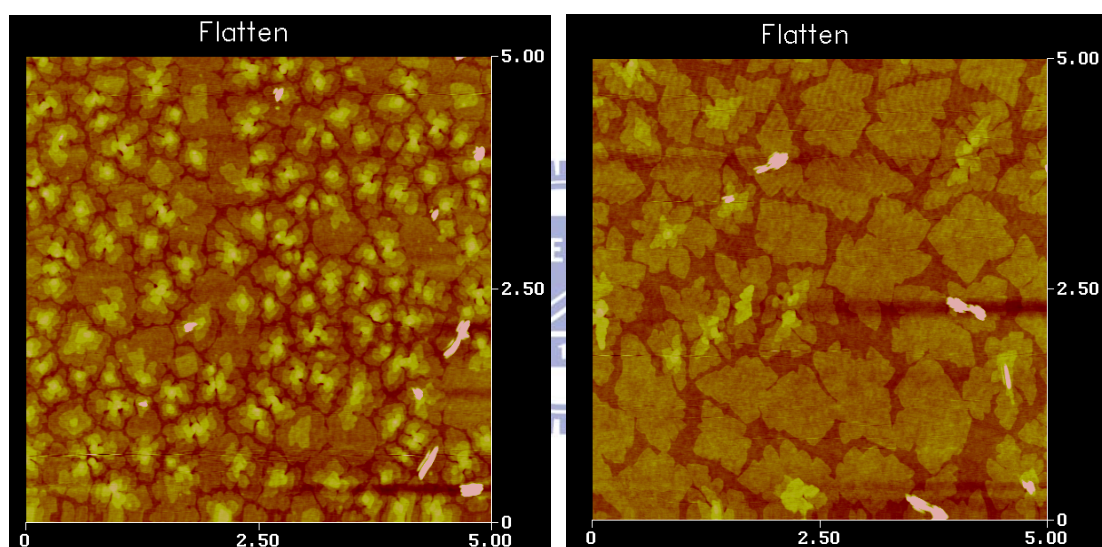
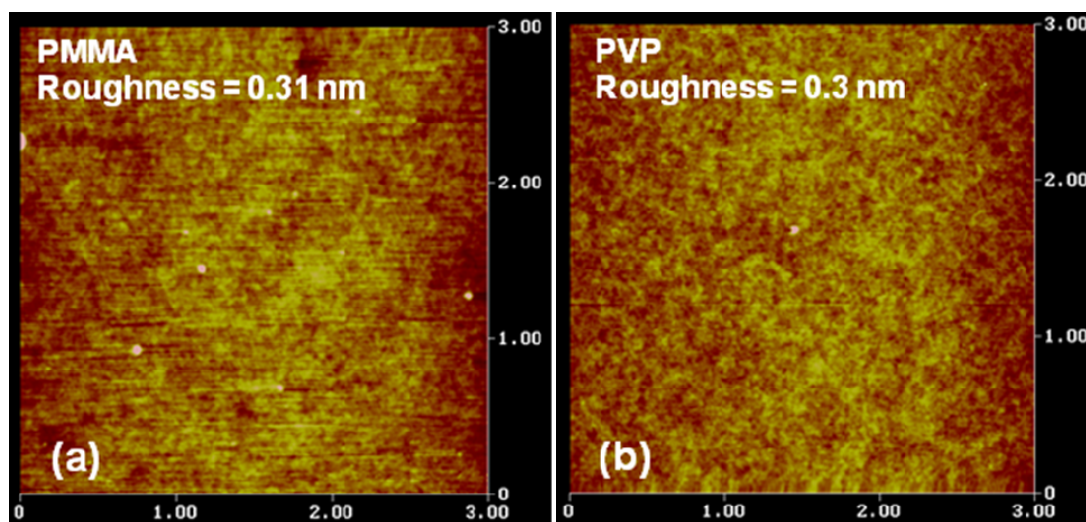


Fig. 3.5 Atomic force microscope (AFM) images of (a) PMMA surface (b) PVP surface, and images of 25 Å pentacene (c) deposit on PMMA dielectric (d) deposit on PVP dielectric

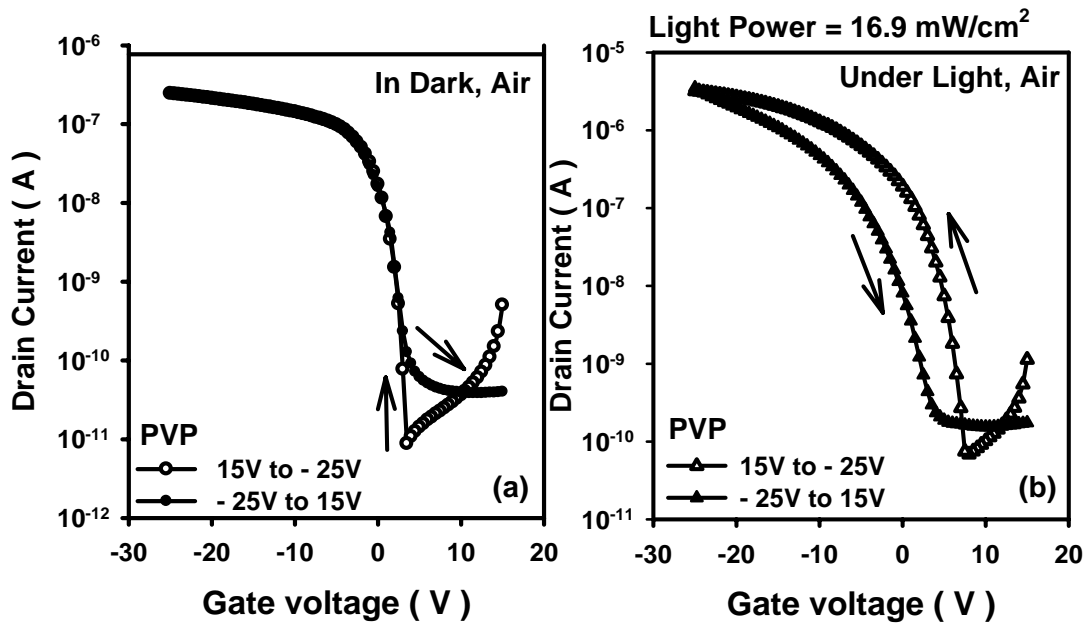


Fig. 3. 6 The transfer characteristic of PVP-OTFTs sweep in both directions under the dark (b) under the light

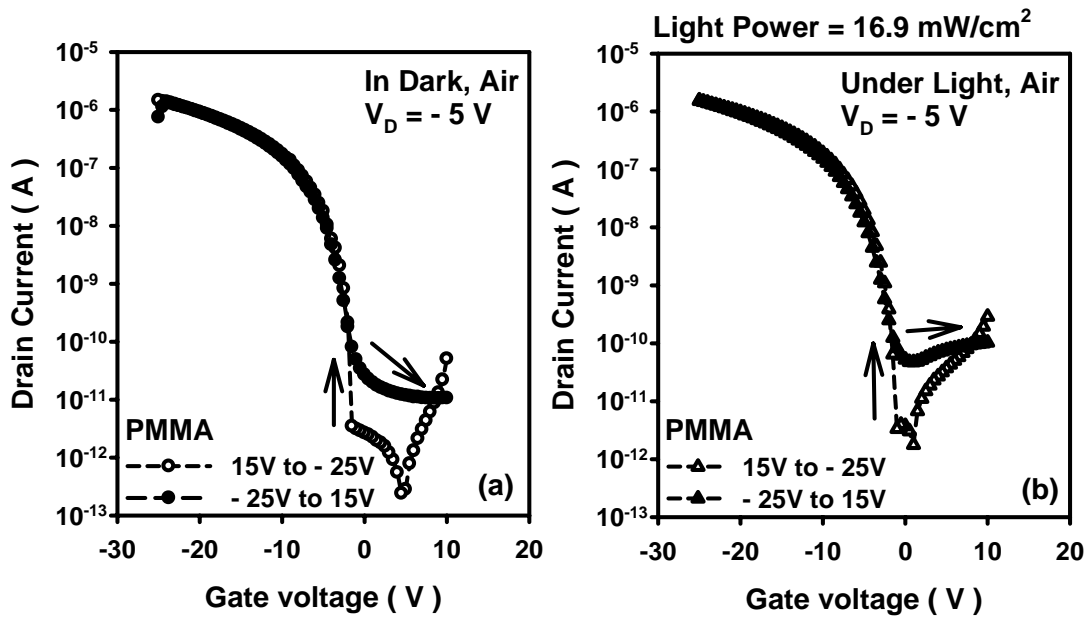


Fig. 3. 7 The transfer characteristic of PMMA-OTFTs sweep in both directions (a) under the dark (b) under the light

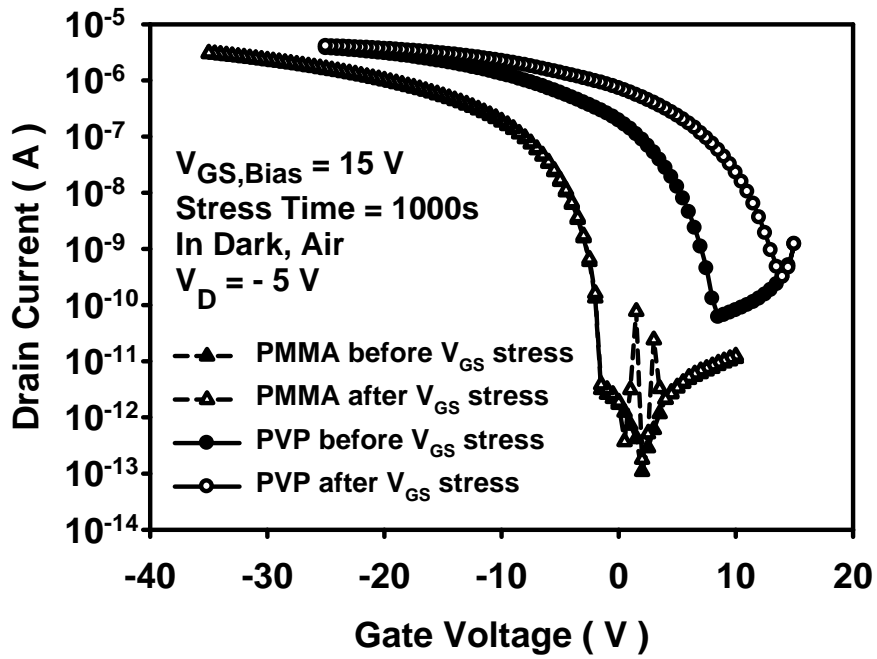


Fig. 3. 8 The linear-region transfer characteristics of devices before and after 1000 second positive gate bias stress

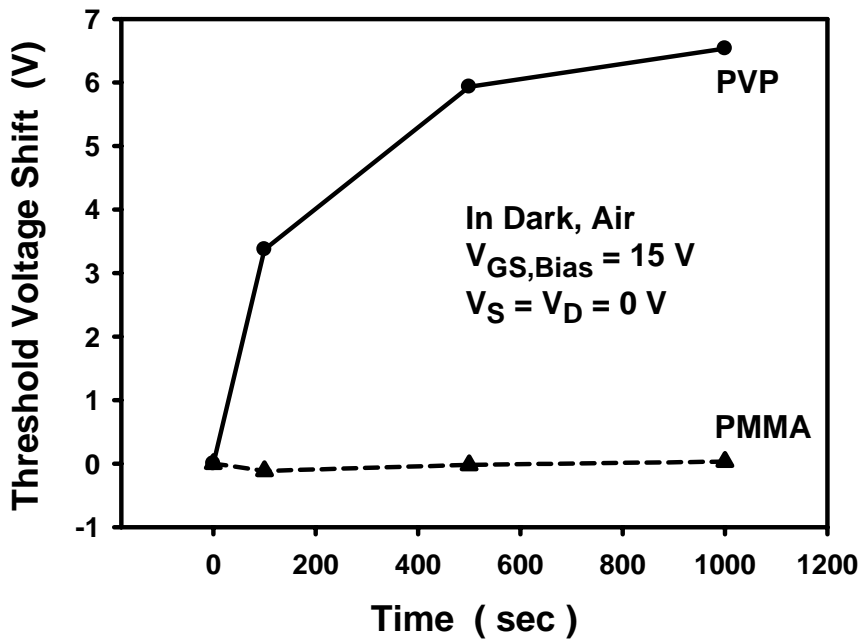


Fig. 3. 9 Threshold voltage shift (ΔV_{th}) of PMMA and PVP devices during positive gate bias stress in dark and air

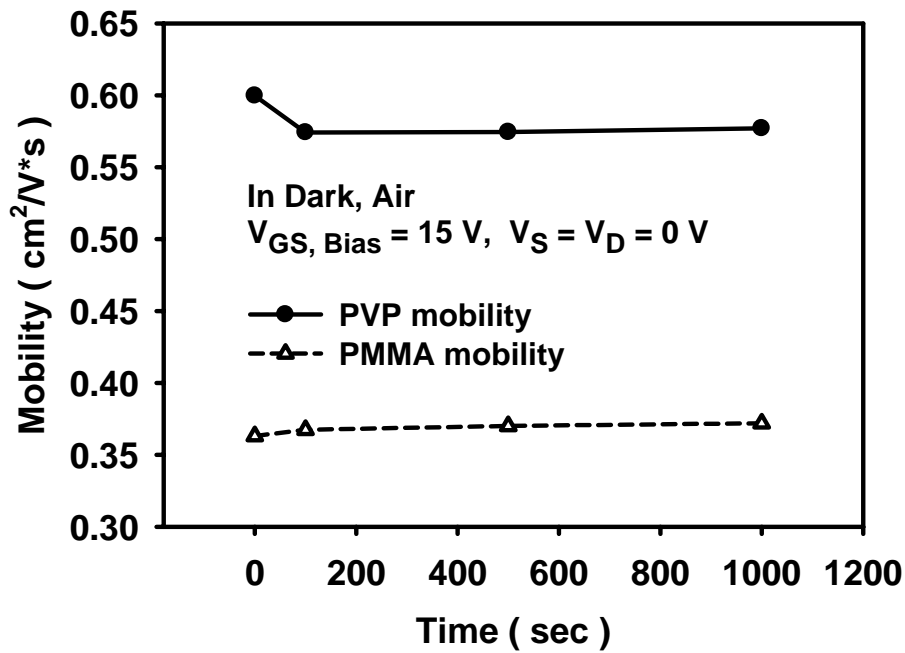


Fig. 3. 10 The field-effect mobility plot as a function of positive bias stress time

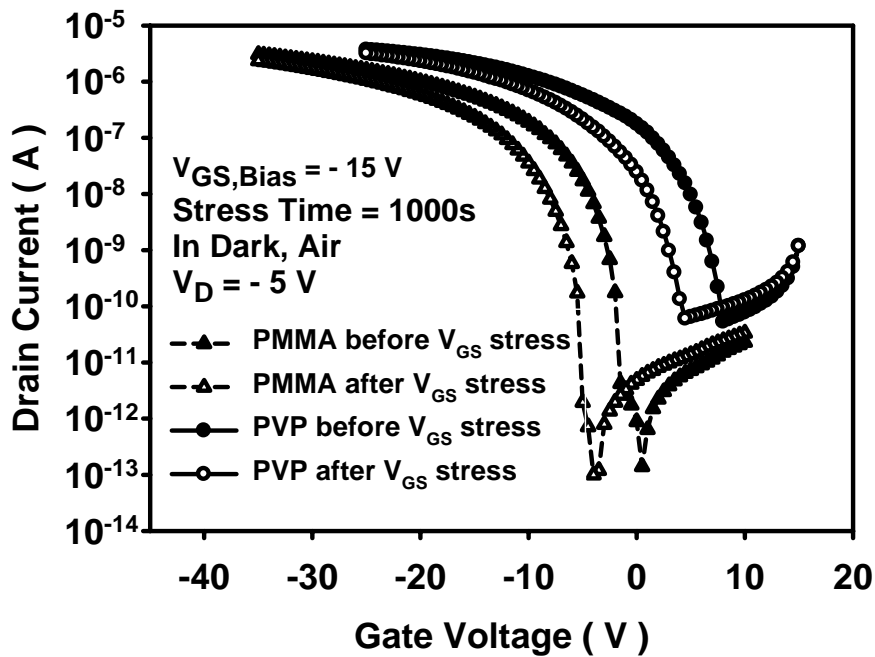


Fig. 3. 11 The linear-region transfer characteristics of devices before and after 1000 second negative gate bias stress

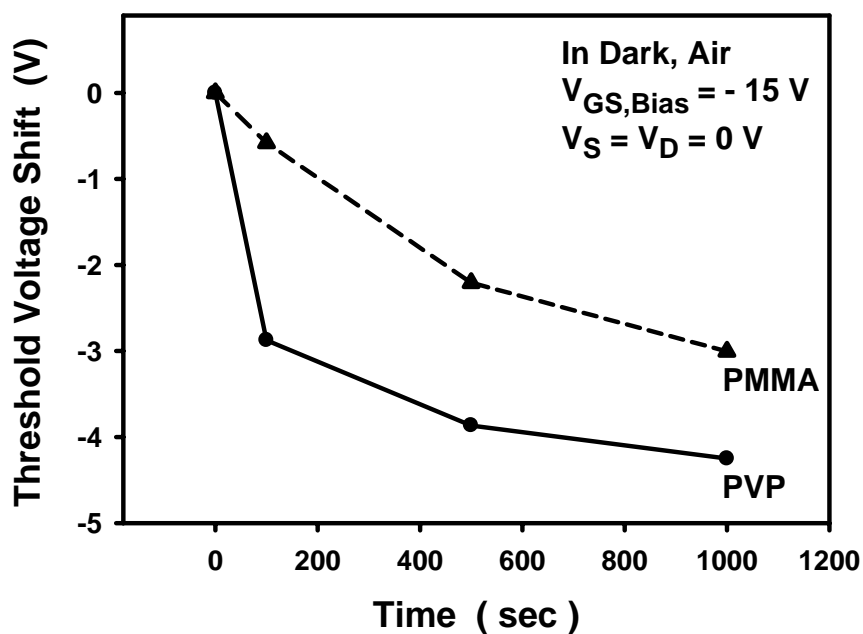


Fig. 3.12 Threshold voltage shift (ΔV_{th}) of PMMA and PVP devices during negative gate bias stress in dark and air

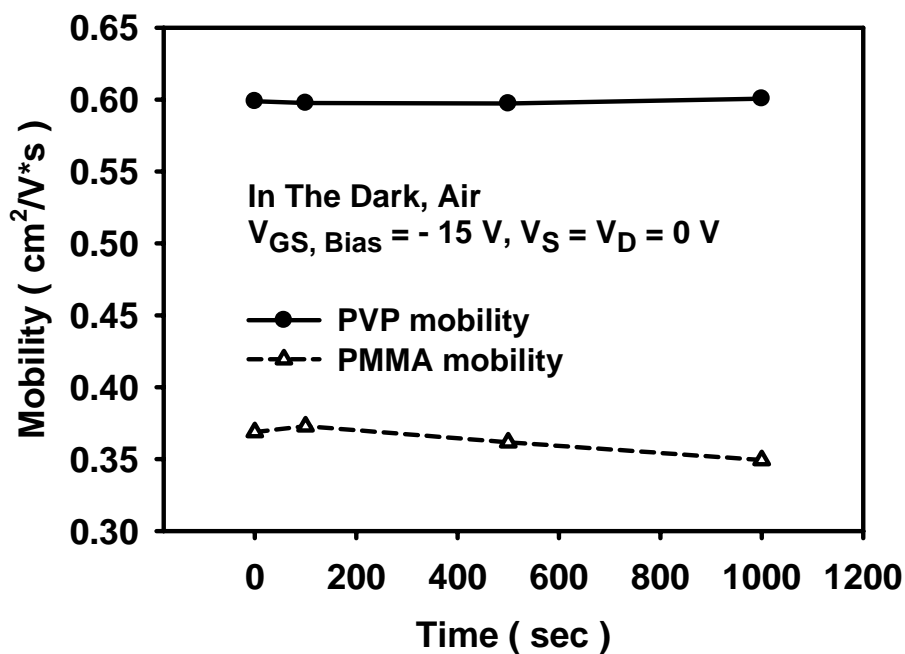


Fig. 3.13 The field-effect mobility plot as a function of negative bias stress time

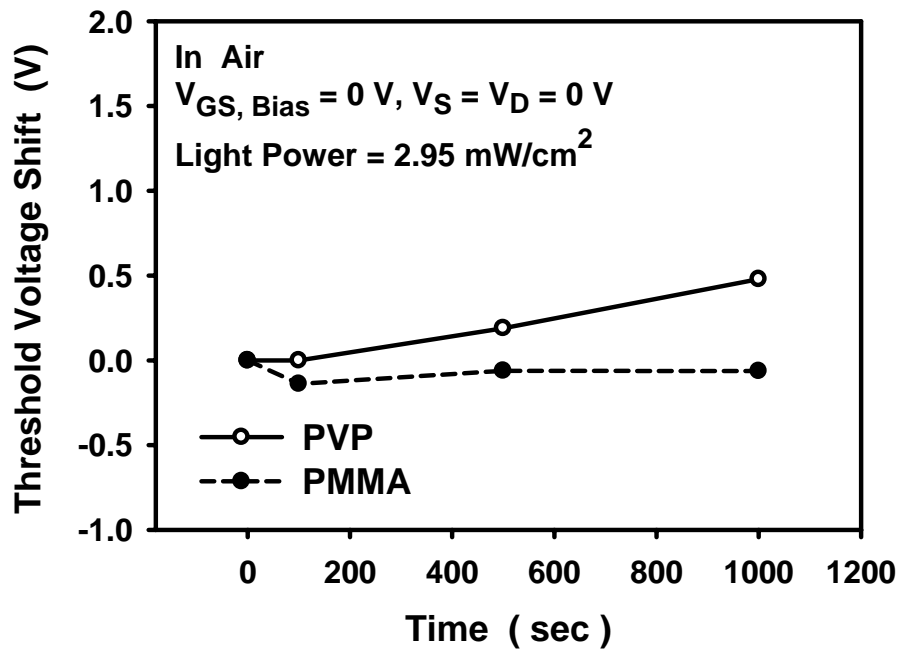


Fig. 3.14 Threshold voltage shift (ΔV_{th}) of PMMA and PVP devices under 2.95 mW/cm^2 illumination

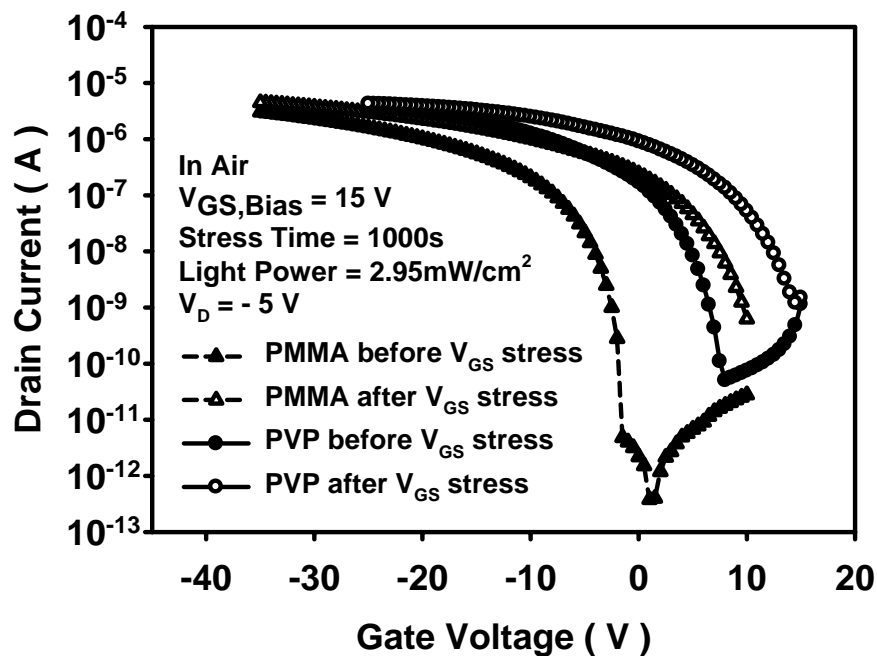


Fig. 3.15 The linear-region transfer characteristics of devices before and after 1000 second positive gate bias stress under illumination

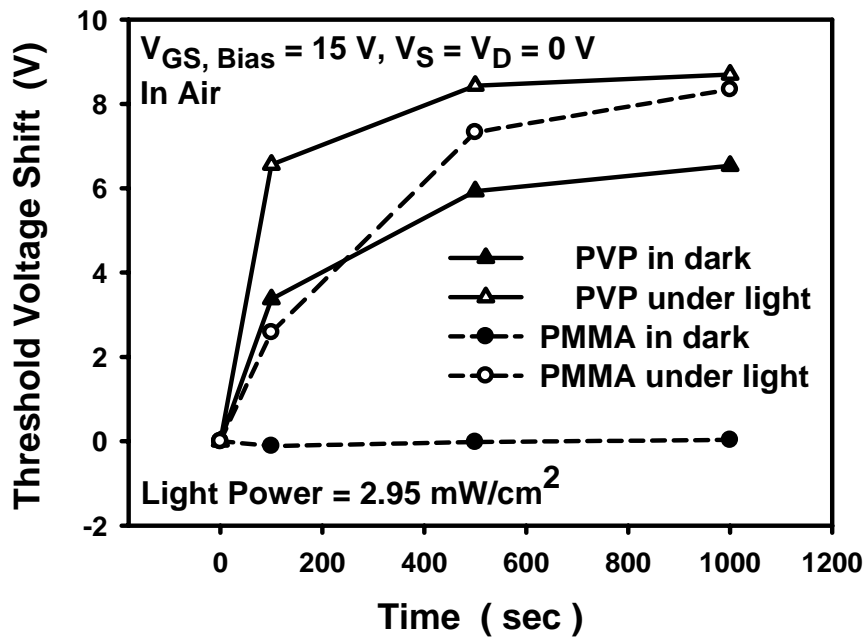


Fig. 3. 16 Threshold voltage shift (ΔV_{th}) of PMMA and PVP devices in dark and under illumination

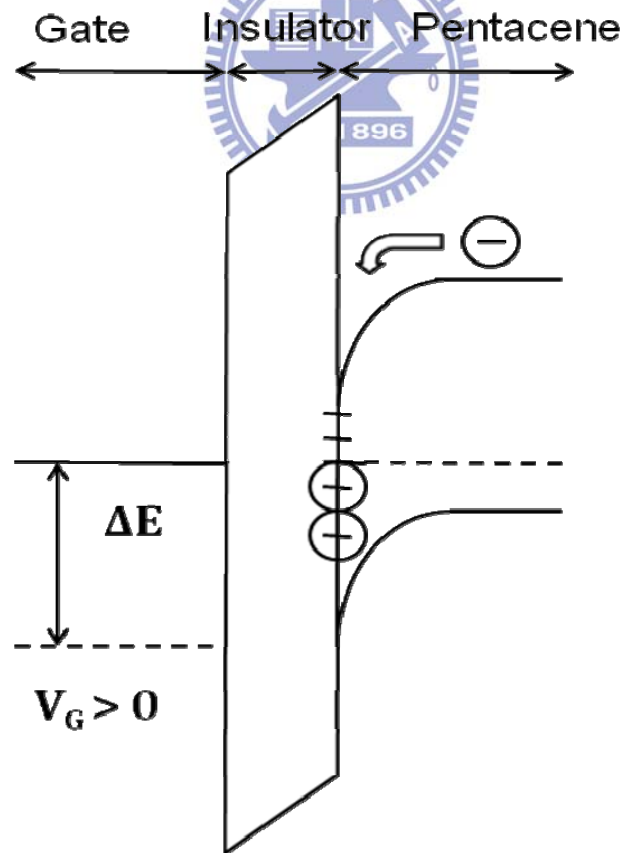


Fig. 3. 17 model of threshold voltage shift controlled by the charge capturing when $V_G > 0$ under illumination

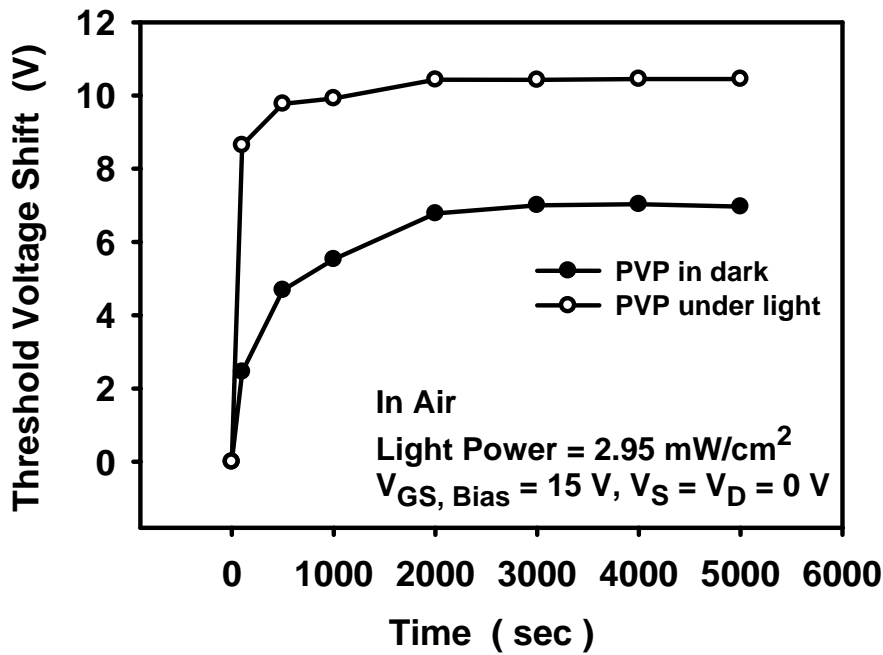


Fig. 3.18 Long time positive bias stress experiment of PVP-OTFTs in dark and under illumination

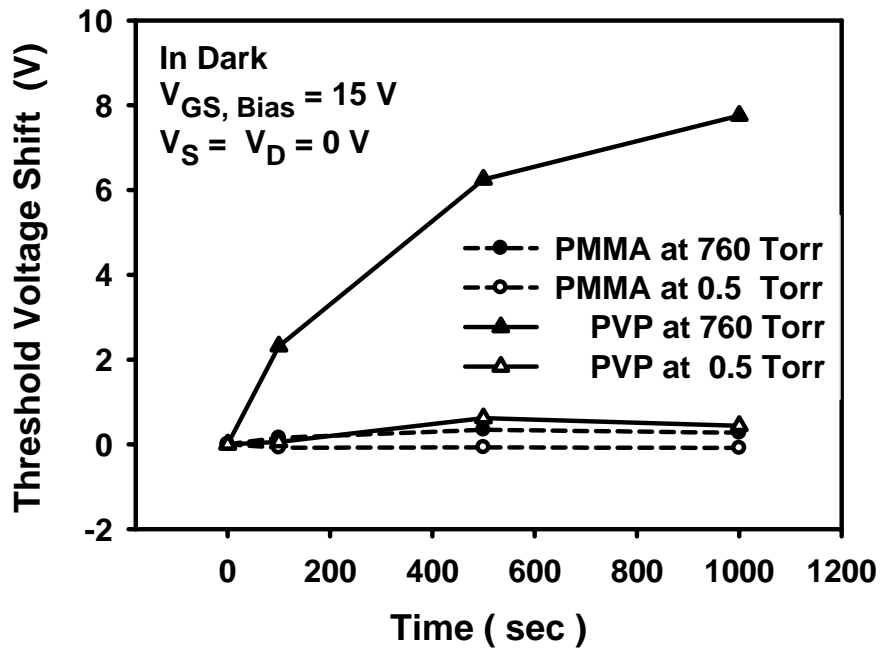


Fig. 3.19 Threshold voltage shift (ΔV_{th}) of PMMA and PVP devices in dark air and dark vacuum

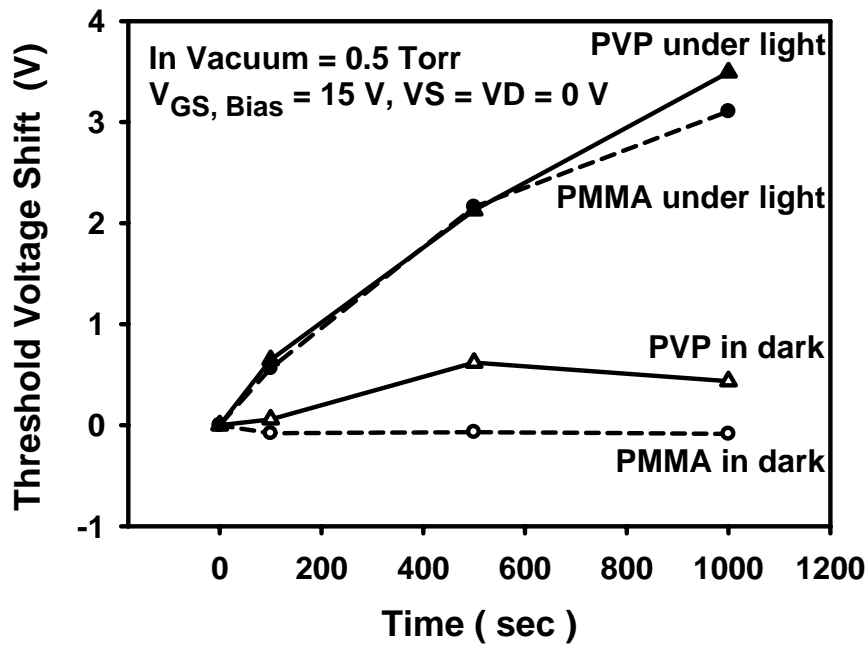


Fig. 3. 20 Threshold voltage shift (ΔV_{th}) of PMMA and PVP devices in dark and under illumination, measurement is taken in vacuum

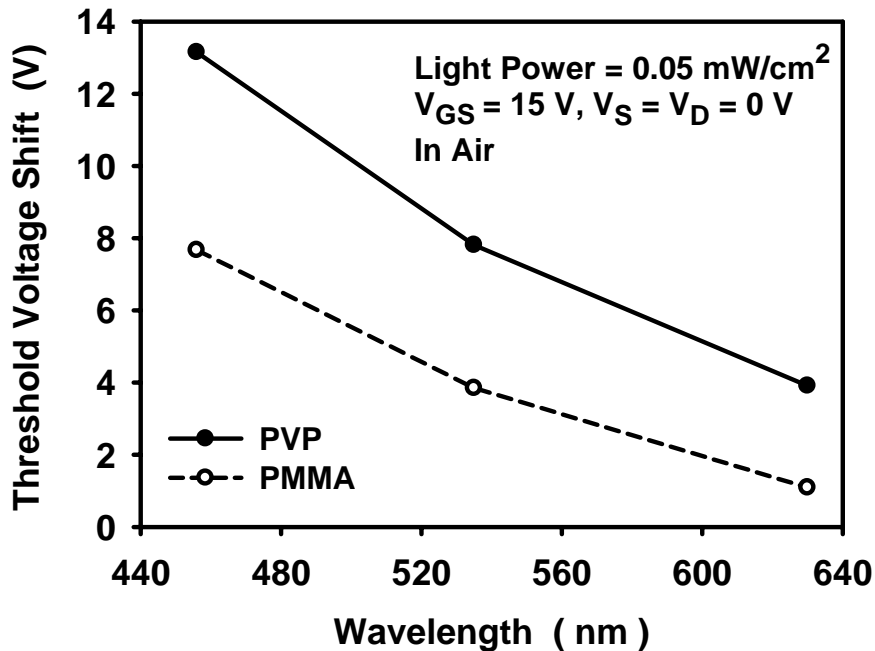


Fig. 3. 21 Threshold voltage shift (ΔV_{th}) of PMMA and PVP devices under different wavelength light illumination

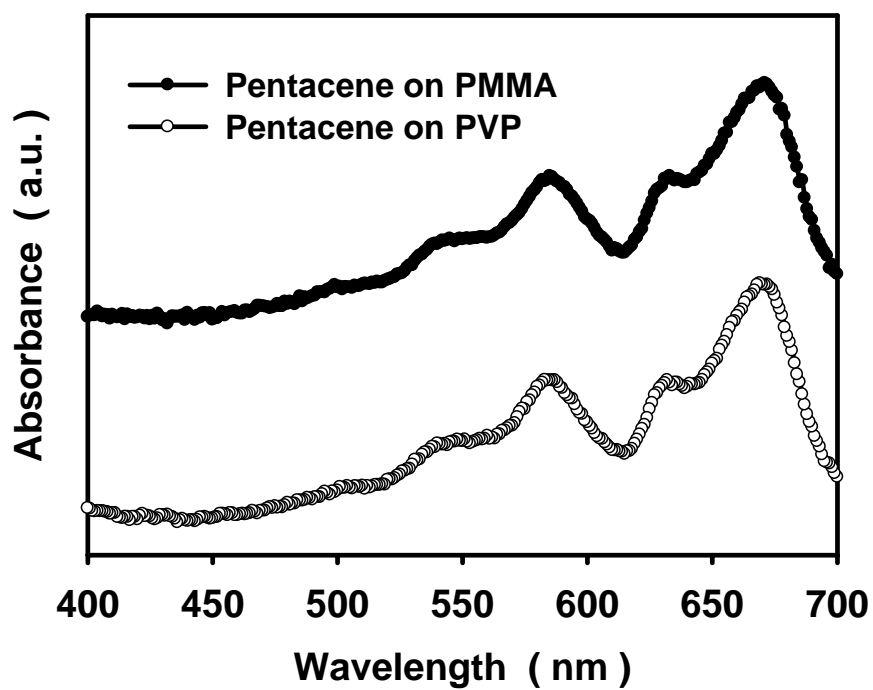
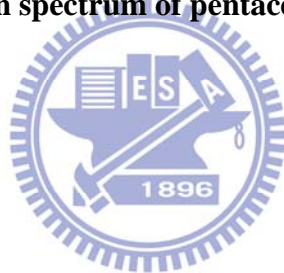


Fig. 3. 22 The absorption spectrum of pentacene on PVP and PMMA film



Chapter 4

Conclusion

In this thesis, we use PVP and PMMA as dielectric surface treatment material and fabricate pentacene-based OTFTs. PVP-OTFTs have OH groups on its interface while PMMA-OTFTs do not. We study how OH groups interact with environment and form carrier traps by comparing these two kinds of OTFTs

Through contact angle system and Fourier transform infrared spectroscopy (FTIR) measurement, OH groups is confirmed existing on PVP-OTFTs. X-ray diffraction (XRD) and atomic force microscope (AFM) then used to examine the crystallization and morphology of pentacene grown on PVP/PMMA. PVP-OTFTs' field-effect mobility ($0.6\text{cm}^2/\text{V}\cdot\text{s}$) was larger than PMMA-OTFTs' ($0.36\text{cm}^2/\text{V}\cdot\text{s}$). This may because pentacene grow on PVP surface have larger grain size.

OH groups can form electron traps and illumination will photogenerate electrons and holes in pentacene. Experiment shown OH groups' short electron-trapping and long electron-releasing time leads hysteresis of PVP-OTFTs in the light.

Except the defects originally form by different pentacene deposition conditions, there are at least two other kinds of defects generated in different measure conditions.

- (i) Pentacene's Fermi level banding induced defects under gate bias stress environment, these defects can be filled by photogenerated carriers and caused ΔV_{th} .
- (ii) OH groups interacted with H_2O and O_2 in the air and become negative charge states, these trap states could cause ΔV_{th} even in the dark environment.

Short life time and poor stability prohibit OTFTs from further use. Base on our result, if OTFTs want to be further applied in driving electric circuits, passivation layer that protect pentacene (or other organic semiconductor) from H_2O and O_2 is

needed. On the other hand, significant ΔV_{th} of PVP-OTFTs and PMMA-OTFTs also implicate their application in moisture/light sensor.



Reference

- [1] Yoshihide Fujiski, Hiroto Sato, Hideo Fujikaki, Youji Inoue, Shizuo Tokito and Taichiro Kurita, Japanese Journal of Applied Physics, Vol. 44, 3728–3732, (2005)
- [2] Yong-Hoon Kim, Sung-Kyu Park, Dae-Gyu Moon, Won-Keun Kim, Jeong-In Han, Displays, Vol. 25, 167–170 (2004)
- [3] Vaibhav Vaidya, Susan Soggs, Jungbae Kim, Andreas Haldi, Joshua N. Haddock, Bernard Kippelen, and Denise M. Wilson, IEEE Transactions on circuits and systems, Vol. 55, No. 5, (2008)
- [4] Tse Nga Ng and John A. Marohn, Journal of Applied Physics, Vol. 100, 084505, (2006)
- [5] Tse Nga Ng, Jürgen H. Daniel, Sanjiv Sambandan, Ana-Claudia Arias, Michael L. Chabinyk, and Robert A. Street, Journal of Applied Physics, Vol. 103, 044506, (2008)
- [6] S. Cipolloni, L. Mariucci, A. Valletta, D. Simeone, F. De Angelis, G. Fortunato, Thin Solid Films Vol. 515, 7546–7550, (2007)
- [7] John E. Northrup and Michael L. Chabinyk, Physical Review B Vol. 68, 041202, (2003)



- [8] Hyun Sook Byun, Yong-Xian Xu, Chung Kun Song, Thin Solid Films Vol. 493,278 – 281, (2005)
- [9] Hagen Klauk, Marcus Halik, Ute Zschieschang, Gu, Journal of Applied Physics, Vol 92, 9, (2002)
- [10] D. K. Hwang, Ji Hoon Park, Jiyoul Lee, Jeong-M. Choi, Jae Hoon Kim, Eugene Kim and Seongil Im, Journal of The Electrochemical Society, Vol. 153, G23-G26 (2006)
- [11] C. M. Chan, Polymer Surface Modification and Characterization (Hanser Gardner, New York, 1994), Chap. 2, p 35.
- [12] Sang Chul Lim, Seong Hyun Kim, Jae Bon Koo, Jung Hun Lee, Chan Hoe Ku, Yong Suk Yang, and Taehyoung Zyung, Apply Physics Letters, Vol. 90, 173512, (2007)
- [13] Se Hyun Kim, Jaeyoung Jang, Hayoung Jeon, Won Min Yun, Sooji Nam, and Chan Eon Park, "Hysteresis-free pentacene field-effect transistors and inverters containing poly(4-vinyl phenol-co-methyl methacrylate) gate dielectrics," Apply Physics Letters, Vol. 92, 183306, (2008)
- [14] G.-W. Kang, K.-M. Park, J.-H. Song, C.H. Lee, D.H. Hwang Current Applied Physics 5, 297–301, (2005)
- [15] Sang Yoon Yang, Kwonwoo Shin, and Eon Park, Advance Functional Materials, Vol. 15, 1806-1814, (2005)

- [16] Yunseok Jang, Do Hwan Kim, Yeong Don Park, Jeong Ho Cho, Minkyu Hwang, and Kilwon Cho, *Apply Physics Letters*, Vol 87, 152105, (2005)
- [17] C. D. Dimitrakopoulos, A. R. Brown and A. Pomp, *Journal of Apply Physics*, Vol. 80, 2501, (1996)
- [18] Chang Bum Park, Takamichi Yokoyama, Tomonori Nishimura, Koji Kita, and Akira Toriumi, *Japanese Journal of Applied Physics*, Vol. 47, 3189–3192, (2008)
- [19] Sangyun Lee, Bonwon Koo, Joonghan Shin, Eunkyong Lee, and Hyunjeong Park, *Apply Physics Letters*, Vol. 88, 162109, (2006)
- [20] D. K. Hwang, Kimoon Lee, Jae Hoon Kim, and Seongil Im, *Apply Physics Letters*, Vol. 89, 093507, (2006)
- [21] X.-H. Zhang, B. Domercq, and B. Kippelen, “High-performance and electrically stable C60 organic field-effect transistors,” *Apply Physics Letters*, Vol. 91, 092114, (2007)
- [22] Tokiyoshi Umeda, Daisuke Kumaki, Shizuo Tokito, *Organic Electronics*, Vol. 9, 545–549, (2008)
- [23] Yan Hu, Guifang Dong, Chen Liu, Liduo Wang, and Yong Qiu, *Apply Physics Letters*, Vol. 89, 072108, (2006)

- [24] Lijuan Zhen, Liwei Shang, Ming Liu, Deyu Tu, Zhuoyu Ji, Xinghua Liu, Ge Liu, Jiang Liu, and Hong Wang, *Apply Physics Letters*, Vol. 93, 203302, (2008)
- [25] Gong Gu, Michael G. Kane, and Siun-Chuon Mau, “Reversible memory effects and acceptor states in pentacene-based organic thin-film transistors,” *Journal of Applied Physics*, Vol. 101, 014504, (2007)
- [26] C. Goldmann, C. Krellner, K. P. Pernstich, S. Haas, D. J. Gundlach, and B. Batlogg, *Journal of Applied Physics*, Vol. 99, 034507, (2006)
- [27] Hsiao-Wen Zan and Shin-Chin Kao, “The Effects of Drain-Bias on the Threshold Voltage Instability in Organic TFTs,” *IEEE Electron Device Letters*, Vol. 29, No.2, (2008)
- [28] Tae Ho Kim, Chang Gi Han, Chung Kun Song, *Thin Solid Films*, Vol. 516, 1232–1236, (2008)
- [29] Maarten Debucquoy, Stijn Verlaak, Soeren Steudel, Kris Myny, Jan Genoe, and Paul Heremans, *Apply Physics Letters*, Vol 91, 103508, (2007)
- [30] Hsiao-Wen Zan and Shih-Chin Kao, *impressed*.
- [31] Chang Bum Park, Takamichi Yokoyama, Tomonori Nishimura, Koji Kita, and Akira Toriumi, *Journal of The Electrochemical Society*, Vol. 155, H575-H581,

(2008)

[32] Gong Gu and Michael G. Kane, *Apply Physics Letters*, Vol 92, 053305, (2008)

[33] Young H. Noh, S. Young Park, Soon-Min Seo, Hong H. Lee, *Organic Electronics*, Vol. 9, 271–275, (2006)

[34] C. Goldmann, D. J. Gundlach, and B. Batlogg, *Apply Physics Letters*, Vol. 88, 063501, (2006)

[35] Fang-Chung Chen and Cheng-Hsiang Liao, *Apply Physics Letters*, Vol. 93, 103310, (2008)



[36] Amare Benor, Arne Hoppe, Veit Wagner, Dietmar Knipp, *Organic Electronics*, Vol. 8, 749–758, (2007)

[37] Daisuke Kumaki, Tokiyoshi Umeda, and Shizuo Tokito, *Apply Physics Letters*, Vol. 92, 093309, (2008)

[38] Yong-Young Noh and Dong-Yu Kim, *Journal of Applied Physics*, Vol. 98, 074505, (2005)
